Soraia Patrícia Caetano da Silva

Licenciatura em Biologia Molecular e Genética

Osteoclastogenesis, inflammatory cytokines and biomarkers of bone metabolism in psoriatic arthritis

Dissertação para obtenção do Grau de Mestre em
Bioquímica para a Saúde

Orientador: Elsa Vieira de Sousa, MD, JEFonseca's Lab, Instituto de Medicina Molecular, Faculdade de Medicina da Universidade de Lisboa

Co-orientador: António Sebastião Rodrigues, PhD,
Faculdade de Ciências Médicas da Universidade Nova de Lisboa

2015

Soraia Patrícia Caetano da Silva

Licenciatura em Biologia Molecular e Genética

Osteoclastogenesis, inflammatory cytokines and biomarkers of bone metabolism in psoriatic arthritis

Dissertação para obtenção do Grau de Mestre em
Bioquímica para a Saúde

Orientador: Elsa Vieira de Sousa, MD, JEFonseca's Lab, Instituto de Medicina Molecular, Faculdade de Medicina da Universidade de Lisboa

Co-orientador: António Sebastião Rodrigues, PhD,
Faculdade de Ciências Médicas da Universidade Nova de Lisboa

Faculdade de Ciências Médicas da Universidade Nova de Lisboa

2015

Osteoclastogenesis, inflammatory cytokines and biomarkers of bone metabolism in psoriatic arthritis

AGRADECIMENTOS

Quero em primeiro lugar agradecer ao Professor João Eurico Fonseca por me ter aceite na Unidade de Investigação em Reumatologia e à minha orientadora Elsa Sousa, por me ter mostrado como a área da reumatologia pode ser tão intrigante e interessante, integrando-me num projeto multidisciplinar.

Ao João Rodrigues, por se ter prontamente disponibilizado a ceder-me as células MG-63 e esclarecer as minhas dúvidas sobre o estabelecimento desta cultura.

À Irina Alho, por não só me ter disponibilizado as células hFOB 1.19, mas também pelo acompanhamento todo ao longo do estabelecimento da cultura de osteoblastos. Obrigada pelas conversas, palavras de incentivo e todo o apoio que me deste ao longo destes meses de altos e baixos.

Agradeço também ao Biobanco-IMM pelas amostras de controlos saudáveis cedidas neste estudo e por algumas colheitas de sangue de doentes. Às meninas do serviço de histologia e ao Vitor Proa que sempre responderam às minhas questões e me ajudaram no trabalho histológico. Aos funcionários do biotério de roedores, em especial à Joana Marques, Dolores Bonaparte, Iolanda Moreira e Carlos Silva, por toda a experiência que partilharam comigo sobre ratinhos e ratos.

À Susana Lopes da Silva, um sincero obrigada, pela disponibilidade de realizar todas as colheitas de sangue, mesmo quando eram em cima da hora e pela simpatia.

Aos meus colegas de laboratório Ana Lopes, Bruno Vidal e Rita Cascão, pelo esclarecimento de dúvidas e ajuda no trabalho prático do dia-a-dia.

Um agradecimento muito especial à Diana Fernandes por toda a ajuda, conselhos e truques que me deu desde o primeiro dia que cheguei à unidade.

À Inês Perpétuo, muito obrigada por me teres mostrado o lado osteoclástico da vida, pelas ideias que me deste, pela paciência em dias menos bons quando os resultados não eram o que se esperava. Porque também foste como uma orientadora para mim, agradeço-te todo o acompanhamento que me deste. Ao longo destes meses de ciência, obrigada também pelas conversas mais geek desde filmes, séries a músicas, sem isso não seria a mesma coisa.

Às meninas de mestrado que estiveram comigo durante toda a tese que partilharam comigo as angústias, os problemas e também as vitórias do trabalho laboratorial. Em especial à Ana Pereira que muito me ensinou sobre ratinhos e que todos os dias trazia uma boa disposição contagiante, obrigada pela cumplicidade e espírito de equipa. À Natacha Leonardo e à Renata Casimiro, pelo companheirismo e momentos de descontração partilhados.

Não posso deixar de agradecer aos meus amigos, que apesar de terem experienciado de longe esta minha aventura, nunca deixaram de me apoiar e acreditar em mim. Um especial obrigada à Cláudia, Maria Inês, Rita, Rui e Viviana, vocês são espetaculares!

Como não podia deixar de ser, agradeço à minha família, em especial aos meus pais, por todo o apoio que me deram, especialmente em alturas que cheguei a duvidar de mim mesma. Por acreditarem desde o início que tudo ia correr bem e que eu ia conseguir. Obrigada por tudo o que têm feito por mim.

Por último, mas não menos importante, um agradecimento aos meus animais: à velhota Amarilis, ao rafeiro Yuri e às princesas Maggie e Nala por conseguirem animar todos os meus dias com muito mimo.

ABSTRACT

Psoriatic arthritis (PsA) is a chronic inflammatory disease characterized by several manifestations involving the joints, enthesis and the skin. New bone formation after inflammation at enthesis site has been one of the most intriguing aspects of the disease. Cellular and molecular mechanisms in this process are still not completely understood.

This study aims to understand better the mechanisms underlying bone formation and resorption and the effect of non-steroid anti-inflammatory drugs (NSAIDs) in these processes. To access that, biomarkers of bone metabolism and inflammatory cytokines were measured in PsA patients' serum before and after NSAID therapy. These selected biomarkers were bone turnover markers such as CTX-I and P1NP, osteoclast differentiation and activation factors RANKL and OPG, Wnt pathway inhibitors DKK-1 and SOST and pro-inflammatory cytokines IL-22, IL-23 and prostaglandin PGE_2. In this context monocyte cell culture was also established after PBMC isolation from PsA patients and healthy controls. Monocytes were cultured *in vitro* under unstimulated and stimulated conditions and two functional assays were performed: TRAP staining and resorption pit assay.

It was demonstrated that CTX-I and OPG serum levels in PsA patients were lower than controls. SOST levels were extremely decreased in comparison with controls, resembling the ankylosing spondylitis patients results already documented. Osteoclast assays confirmed the need of RANKL in stimulating osteoclastogenesis and that celecoxib seems to have an inhibitor role in this process.

The results obtained suggest that PsA patient population analyzed in this study have low bone resorption levels and some bone formation activity.

RESUMO

A artrite psoriática (AP) é uma doença inflamatória crónica caracterizada por várias manifestações nas articulações, nas enteses e na pele. A formação de novo osso após inflamação nas enteses é um dos aspetos mais intrigantes desta doença. Os mecanismos celulares e moleculares deste processo ainda não são completamente conhecidos.

Este estudo tem como objetivo compreender melhor os mecanismos subjacentes à formação e reabsorção óssea, bem como o efeito de anti-inflamatórios não esteroides (AINEs) nestes processos. Para atingir este objetivo foram quantificados biomarcadores do metabolismo ósseo e citocinas inflamatórias em doentes AP, antes e após terapêutica com AINEs. Os biomarcadores selecionados foram marcadores de remodelação óssea como CTX-I e P1NP, fatores de diferenciação e ativação de osteoclastos como o RANKL e a OPG, inibidores da via de sinalização Wnt, nomeadamente o DKK-1 e a SOST e ainda citocinas pro-inflamatórias como a IL-22 e a IL-23 e a prostaglandina PGE_2. Neste contexto foram também estabelecidas culturas celulares de monócitos, isoladas de doentes AP e de controlos saudáveis. Os monócitos foram cultivados *in vitro* em condições não estimuladas e estimuladas e realizados dois ensaios funcionais: coloração com TRAP e ensaio de reabsorção.

Foi observada uma diminuição nos níveis séricos de CTX-I e OPG em doentes AP em relação aos controlos. De igual forma os níveis séricos de SOST encontram-se significativamente mais baixos, em comparação com os controlos saudáveis. Estes valores de SOST são semelhantes aos dos doentes com espondilite anquilosante (EA), documentados anteriormente. Os ensaios com osteoclastos confirmaram a necessidade da presença de RANKL para estimulação da osteoclastogénese e que o celecoxib parece ter um papel inibitório neste processo.

Os resultados obtidos sugerem que a população de doentes com AP analisados têm baixos níveis de reabsorção óssea e alguma atividade na formação óssea.

TABLE OF CONTENTS

INDEX OF FIGURES

INDEX OF TABLES

ABBREVIATIONS

AS	Ankylosing spondylitis
ALP	Alkaline phosphatase
BMD	Bone mineral density
BMP	Bone morphogenetic protein
CASPAR	Classification criteria for psoriatic arthritis
CCP	Cyclic-citrullinated peptide
cDNA	Complementary DNA
CIA	Collagen induced arthritis
CO_2	Carbon dioxide
COX	Cyclooxygenase
CRP	C-reactive protein
CSF1R	Colony stimulating factor 1 receptor
Ct	Cycle treshold
CTX-I	C-terminal telopeptide I
DAB	3,3'-diaminobenzidine
DC	Dendritic cell
DIP	Distal interphalangeal predominant
DKK-1	Dickkopf-related protein 1
DMARD	Disease-modifying anti-rheumatic drug
DMEM	Dulbecco's Modified Eagle's medium
DMSO	Dimethyl sulfoxide
DNA	Deoxyribonucleic acid
ELISA	Enzyme-linked immunosorbent assay
ESR	Erythrocyte sedimentation rate
FBS	Fetal bovine serum
Fig.	Figure
HEPES	4-(2-hydroxyethyl)-1-piperazineethanesulfonic acid
H&E	Hematoxylin and eosin
H^+	Proton

HLA	Human leukocyte antigen
HRP	Horse radish peroxidase
HSC	Hematopoietic stem cell
IBD	Inflammatory bowel disease
IHC	Immunohistochemistry
IL	Interleukin
ILC	Innate lymphoid cell
JAK1	Janus kinase 1
LTi	Lymphoid tissue inducer
MAPK	Mitogen-activated protein kinase
MCP-1	Monocyte chemotactic protein-1
M-CSF	Macrophage colony-stimulating factor
MHC	Major histocompatibility complex
MSC	Mesenchimal stem cell
mTNF	Membrane bound tumor necrosis factor
MTT	3-(4,5-Dimethylthiazol-2-yl)-2,5-Diphenyltetrazolium Bromide
NFATc1	Nuclear factor of activated T cells cytoplasmic 1
NF-kB	Nuclear factor kappa-light-chain-enhancer of activated B cells
lsNK	Natural killer
NSAID	Nonsteroidal anti-inflammatory drug
NTC	No template control
OA	Osteoarthritis
OB	Osteoblast
OC	Osteoclast
OCN	Osteocalcin
OCY	Osteocyte
OPG	Osteoprotegerin
OSX	Osterix
P1CP	Procollagen type 1 C propeptide
P1NP	Procollagen type 1 N propeptide
PBMC	Peripheral blood mononuclear cell

PBS	Phosphate buffered saline
pH	Negative logarithm for hydrogen ion
PGE_2	Prostaglandin E2
Pre-OC	Pre-osteoclast
Ps	Psoriasis
PsA	Psoriatic arthritis
PTH	Parathyroid hormone
qPCR	Quantitative polymerase chain reaction
RA	Rheumatoid arthritis
RANK	Receptor activator of nuclear factor-kB
RANKL	Receptor activator of nuclear factor kappa-B ligand
RF	Rheumatoid factor
RGD	Arginylglycylaspartic acid
RNA	Ribonucleic acid
RORγt	Retinoic acid-related oprhan receptor γ
RPMI	Roswell Park Memorial Institute
rRNA	Ribosomal ribonucleic acid
RT-PCR	Reverse transcription polymerase chain reaction
SNP	Single nucleotide polymorphism
SOST	Sclerostin
SpA	Spondyloarthritis
SPF	Specific pathogen free
STAT3	Signal transducer and activator of transcription 3
TBE	Tris/Borate/EDTA
TE	Tris/EDTA
TNF	Tumor necrosis factor
TRAP	Tartrate-resistant acid phosphatase
TYK2	Tyrosine kinase 2
Wnt	Wingless
WT	Wild-type

INTRODUCTION

Psoriatic Arthritis

Psoriatic arthritis (PsA) is a chronic inflammatory disease characterized by several manifestations involving the joints, enthesis and the skin. In PsA, the enthesis has been recognized as a central and functional pathogenic organ (Fig. 1). New bone formation was documented at the enthesis were previous inflammation was detected. Concomitantly, inflammation occurs at the adjacent synovium tissue and increases synovial liquid production which results in swollen joints. Nevertheless the cellular and molecular pathways involved in this process are not well understood (Alvarez-Nemegyei and Canoso 2006).

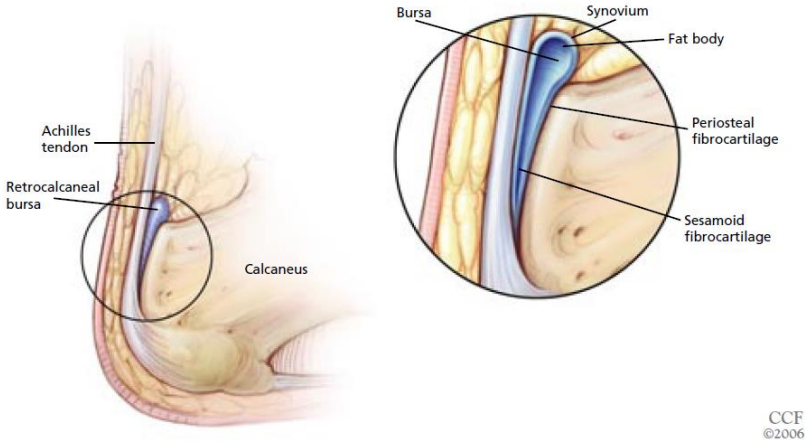

Fig. 1 – Representation of the entheseal organ (Adapted from Alvarez-Nemegyei & Canoso, 2006).

People of all ages can be affected by this disease, but its major incidence is in young adults. The diagnose is established mainly between 15-35 years old and the gender ratio is 1:1.3, being a little more common in women (Amherd-Hoekstra et al. 2010).

Although generally a seronegative rheumatoid factor (RF) spondyloarthritis, in some patients resembles rheumatoid arthritis (RA), another inflammatory joint disease, which makes it difficult to diagnose (Amherd-Hoekstra et al. 2010), (Duarte, Faillace, and Freire de Carvalho 2012), (Gladman et al. 2005).

Differential diagnosis with RA is based in the presence of the RF although about 13% of PsA might be RF positive (Duarte, Faillace, and Freire de Carvalho 2012). In alternative cyclic citrullinated peptide (CCP) antibody test which is highly specific for RA can confirm the diagnosis. (Bas et al. 2003).

Prevalence and incidence

PsA shows ethnic and geographic variations, being more common in the colder north than in the tropics. PsA prevalence is higher in Europe and lower in Japan (Chandran and Raychaudhuri 2010).

In Europe there are different prevalences depending on the regions. That could be explained by ethnic variation, heterogeneity in study methods and difficulties with PsA classification. The prevalence ranges between 0.02% in Sweden and 0.42% in Italy. In the USA the estimated prevalence is 0.25%. Japan continues to have the lowest prevalence in the globe with only 0.00001%. In China the prevalence ranges between 0.01 and 0.1%. It was also reported a prevalence of 0.47% in Australia Aboriginal community (Chandran and Raychaudhuri 2010).

Another important estimative is the prevalence of patients that develop PsA once they have psoriasis (Ps). This percentage is very variable, it depends on many factors. Thus the range could be from 6 to 42%. If we study specific populations such as Italian patients, one can have a percentage between 7.7 to 36% (Chandran and Raychaudhuri 2010).

An international study with clinics from UK, Italy, France, Spain and Germany, showed that PsA prevalence increases with time since the diagnosis of psoriasis reaching 20.5% after 30 years. In other independent study in UK, PsA prevalence was 13.8%. The PsA incidence in Europe and USA is 3 to 23.1 cases/100 000, meanwhile in Japan is only 0.1 cases/100 000. It seems that PsA incidence is increasing through the years (Chandran and Raychaudhuri 2010). Although there are many studies documented, the exact prevalence and incidence of PsA are unknown. This could be due to the criteria used to classify PsA and to incorrect classification, even specialists find this task difficult sometimes.

Symptoms and disease assessment

PsA can appear after, before or without the manifestation of skin disease-psoriasis. In 40% of the cases, patients also have the spinal column affected with spondylarthritis and sacroiliitis. PsA patients have manifestation at insertions of tendons, ligaments and capsules named enthesopathy. The insertion of Achilles tendon is the most commonly affected enthesis (Amherd-Hoekstra et al. 2010). Other symptoms involve joint deformation and destruction of joint cartilage and bone. In PsA osteoproliferation coexists at the same time with bone destruction. In this point PsA differs from RA where only erosive disease can be found. Furthermore, this disease is not exclusive of the joints, it can have as well extraarticular manisfestations such as uveitis.

Diagnosing PsA as quickly as possible is very important in order to give patients the right treatment. Diagnose can be made by searching for the common symptoms of PsA and by magnetic resonance or ultrasound exams when required. Skin biopsies, joint fluid and blood samples can be conducted as well to rule out other diseases. (Duarte, Faillace, and Freire de Carvalho 2012).

Genetic and environmental factors

Environmental risk in this pathology involves streptococcal pharyngitis, daily life stress, low humidity, drugs, HIV infection, trauma, smoking and obesity. Beyond that other associations have been demonstrated, as rubella vaccination, moving house, and HIV infection. Smoking has an interesting role in this disease. The time to develop PsA decreases with smoking, if psoriasis is not present, but when psoriasis is already present smoking increases PsA development time. IL13 gene polymorphisms are responsible for this behavior (Duffin et al. 2009), (Duarte, Faillace, and Freire de Carvalho 2012), (Chandran and Raychaudhuri 2010).

Various studies regarding PsA genetic factors seem to agree that this disease has a strong genetic component. The most common mode of inheritance is a polygenic or multifactorial pattern. It was detected that the recurrence risk for affected first degree relatives is 30.4%. HLA genes, in specific HLA-B27 and HLA-B7 are associated with PsA and not with psoriasis. The association with HLA-B27 is stronger in patients with

sacroiliitis or with distal interphalangeal predominant (DIP) (Chandran and Raychaudhuri 2010), (Barton 2002).

Classification

Nowadays the new criteria for PsA classification are based on CASPAR, Classification of Psoriatic Arthritis Criteria. These criteria have a sensitivity of 0.914 and a specificity of 0.987. The diagnostic criteria of Moll and Wright were widely used for its simplicity and efficacy but CASPAR criteria seem to have more specificity (Helliwell and Taylor 2005), (Wilson et al. 2009).

First of all, patients must have inflammatory articular disease (joints, axial involvement and enthesis) before CASPAR criteria can be applied. In order to fulfill CASPAR criteria patients must present 3 points from the 5 categories present in Table I in ANNEX I.

Treatment

Nowadays there is still no cure for PsA, thus the goal ought to reduce joint pain and swelling, preserve joint function and control skin psoriasis. Treatment strategies will depend on the severity of the disease. Non-steroidal anti-inflammatory drugs (NSAIDs) are commonly the first line of treatment, since it reduces pain, swelling and inflammation. However this kind of treatment can cause stomach distress and ulcers and may increase the risk of heart attack. In mild forms nonsteroidal anti-inflammatory drugs can be associated with a good symptomatic response. Oral and injectable corticosteroids can control inflammation, but its use is generally not recommended for long term. These agents can be co-administrated with intraarticular glucocorticoid injection. Moderate to severe forms receive the same treatment with the addition of disease-modifying antirheumatic drugs (DMARDs) such as methotrexate, sulfasalazine, ciclosporin A, and leflunomide. In refractory cases usually anti-TNF drugs are used such as adalimumab, etanercept, infliximab and golimumab. These medicines are effective on joints or skin, although response might vary from patient to patient. (Amherd-Hoekstra et al. 2010), (Duarte, Faillace, and Freire de Carvalho 2012).

An important NSAID frequently used is celecoxib. This drug is a cyclooxygenase-2 (COX-2) specific inhibitor. Prostaglandins are relevant mediators of many physiological processes and are derived from arachidonic acid via COX pathway (Tive 2000). Prostaglandin E2 (PGE_2) plays an important role in this pathway, since it regulates many aspects in inflammation and functions of different immune cells. PGE_2 can promote the activation, maturation and migration of dendritic cells (DCs), having a pro-inflammatory activity. This prostaglandin is produced by fibroblasts, epithelial cells and infiltrating inflammatory cells (Kalinski 2012). Currently it is known that NSAIDS can inhibit the conversion of arachidonic acid into prostaglandins by COX inhibition. COX has 2 isoforms, COX-1 and COX-2. COX-1 is constitutively expressed since it has physiological functions and COX-2 is only expressed in inflammatory context. Celecoxib has the capacity to specific inhibit the COX-2 isoform only, reducing inflammation on patients (Tive 2000).

Bone structure: osteoblasts, osteocytes and osteoclasts

Bone is a dynamic mineralized tissue that allows locomotion, support and protection of body soft tissues. The three main constituent cells are osteoblasts, osteoclasts and osteocytes. If in one hand osteoblasts are responsible for bone formation, on the other hand they also stimulate osteoclasts that resorb bone. Osteocytes derive from osteoblasts and constitute the majority of bone architecture (Florencio-silva et al. 2015), (Raggatt and Partridge 2010).

Osteoblasts (OBs) are cuboid cells located at the bone surface. These cells derive from mesenchymal stem cells (MSC) as shown in Fig. 2. In the differentiation process, MSCs need to express specific genes that are essential to osteoblast development such as Osterix (OSX). Bone morphogenetic proteins (BMPs) and Wingless (Wnt) pathway intervenients are also required. Once the commitment is established, osteoprogenitor cells start to proliferate and then pre-osteoblasts are formed. Between pre-osteoblasts and osteoblasts a maturation phase takes place. Maturation requires crucial genes like RUNX2 and COL1A and in this transition osteocalcin (OCN), a bone matrix protein, starts to be synthetized. After this, osteoblasts can start to form bone. Bone formation is a two-step process: the first is the deposition of organic matrix and the second its

mineralization. Afterwards osteoblasts can undergo apoptosis or become osteocytes (Florencio-silva et al. 2015), (Raggatt and Partridge 2010).

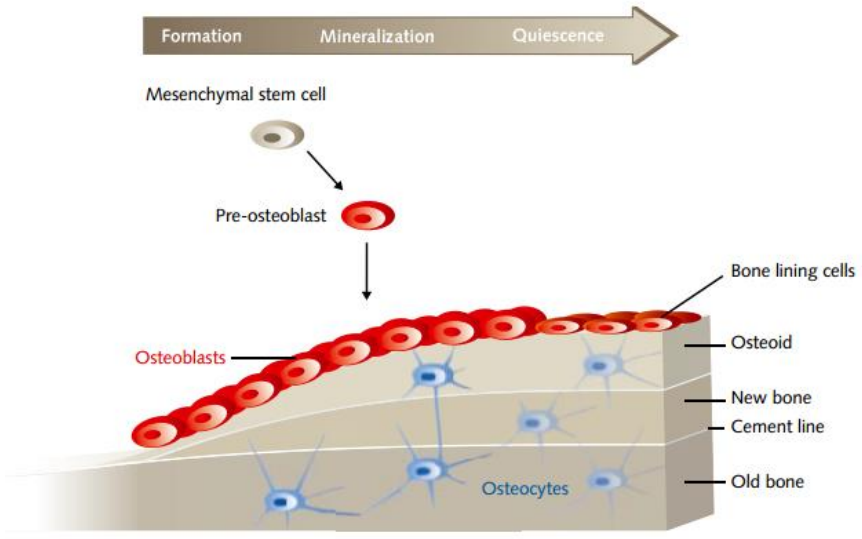

Fig. 2 – Osteoblast development (Adapted from Osteoblast Differentiation and Mineralization, PromoCell).

Osteocytes (OCY) are the most abundant cells in bone architecture, they represent 90-95% of total bone cells. These cells are located in the lacunae and present a dendritic morphology. As described before osteocytes derive from MSC lineage through osteoblast differentiation and have four differentiation stages: osteoid-osteocyte, pre-osteocyte, young osteocyte and mature osteocyte. Everytime a bone formation cycle takes place, some osteoblasts become osteocytes that incorporate into the bone matrix. This process can take up to 6 months. In mature osteocyte stage, the osteoblast markers such as OCN and COL1A are downregulated in contrast with osteocyte markers like sclerostin (SOST) that become expressed. Dickkopf-1 (DKK-1) is also very important, since it is a soluble inhibitor of Wnt pathway (Pinzone et al. 2014). Osteocytes have mechanosensitive functions that allow the detection of mechanical pressure and load, which helps the bone to adapt to daily mechanical forces. These functions are possible due to osteocytes position and network that allows bone cell communication (Florencio-silva et al. 2015), (Raggatt and Partridge 2010).

Osteoclasts (OCs) derive from mononuclear cells of the hematopoietic stem cell (HSC) lineage. To undergo differentiation, osteoclastogenic factors must be present. Macrophage colony-stimulating factor (M-CSF) and receptor activator of NF-ĸB ligand

(RANKL) are the most important ones (Fig. 3). M-CSF is secreted by osteoprogenitor mesenchymal cells and osteoblasts and RANKL by osteoblasts, osteocytes and stromal cells. (Florencio-silva et al. 2015), (Raggatt and Partridge 2010), (Cappariello et al. 2014).

M-CSF acts by binding to its receptor (cFMS) which is present in osteoclast precursors and then stimulates their proliferation and inhibits apoptosis. RANKL is important to osteoclastogenesis. When it binds to its receptor RANK in osteoclast precursors, osteoclast formation is induced. Osteoprotegerin (OPG) is another factor that is produced by OBs and stromal cells. OPG can bind to RANKL and prevent RANK/RANKL interaction, this results in osteoclastogenesis inhibition (Florencio-silva et al. 2015), (Raggatt and Partridge 2010), (Cappariello et al. 2014).

Abnormal increase in osteoclast formation can lead to bone diseases such as osteoporosis, since the ratio bone formation/resorption is not balanced. Osteoclastogenesis deregulation can be a consequence of inflammatory arthritis causing erosions and systemic bone loss (Florencio-silva et al. 2015). If an increase in osteoclastogenesis causes severe damage, an increase in osteoblastogenesis is also as bad. Once osteoblastogenesis is higher than osteoclastogenesis, new bone formation takes place and can be very serious in terms of locomotion, for example bone formation at the enthesis, which sometimes happens in PsA patients.

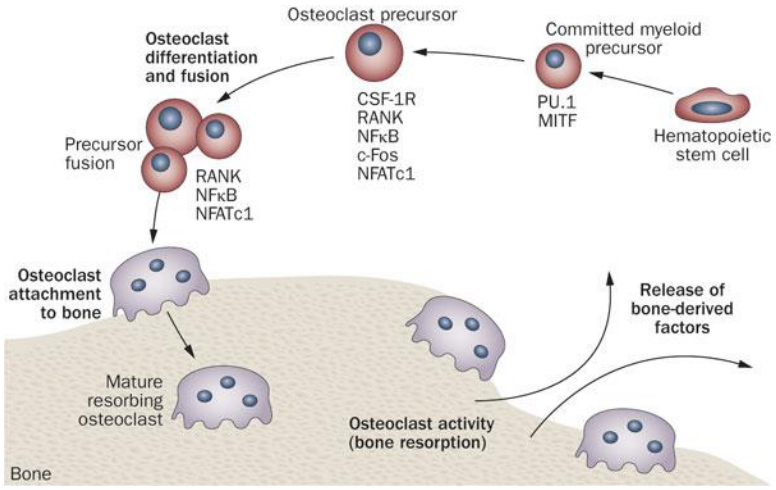

Fig. 3 – Osteoclast development and activity (Adapted from Edwards and Mundy, 2011).

Bone remodeling: a dynamic continuous process

Bone remodeling is a continuous process in life. In equilibrium, bone resorption and formation are well balanced in order to replace old bone by new tissue that can adapt to mechanical load (Florencio-silva et al. 2015), (Raggatt and Partridge 2010), (Hadjidakis and Androulakis 2006). This process depends on OBs, OCYs and OCs and is divided in five phases represented in Fig. 4.

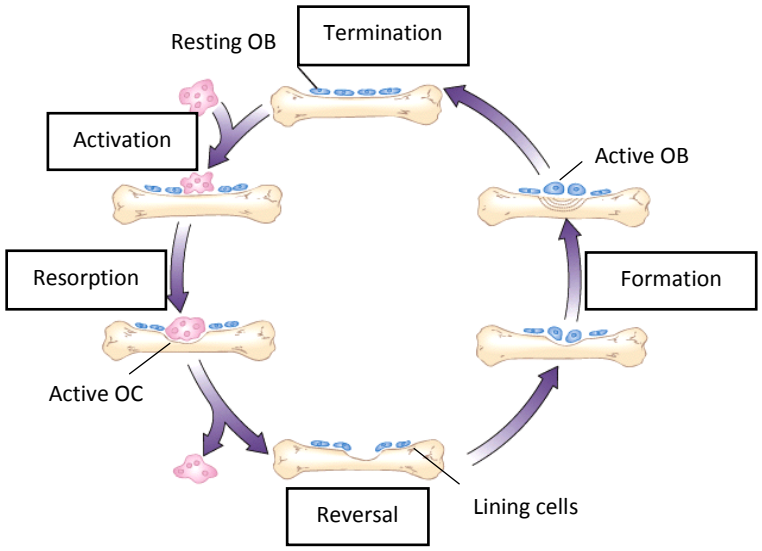

Fig. 4 – Bone remodeling process (Adapted from Wiley).

1. Activation: Before the activation, bone lining cells cover the bone surface. Then the endocrine bone remodeling signal, parathyroid hormone (PTH), binds to the PTH receptor present in pre-osteoblasts (Raggatt and Partridge 2010).

2. Resorption (2 weeks): pre-osteoclasts start to migrate to the bone surface where they form multinucleated osteoclasts. This happens in response to the PTH signaling, that promotes monocyte chemoattractant protein-1 (MCP-1) release from osteoblasts and recruits pre-osteoclasts. OPG expression is decreased at this phase and the production of M-CSF and RANKL increases to promote osteoclast maturation. After this, osteoclasts attach to the RGD (arginylglycylaspartic acid)-binding sites to create a localized microenvironment (sealed zone) that facilitates bone matrix degradation. Bone matrix degradation is possible due to collagenolytic enzymes with low pH such as cathepsin K and

to hydrogen ions that are pumped into the sealed zone (Raggatt and Partridge 2010), (Cappariello et al. 2014).

3. Reversal/Transition (4-5 weeks): Mononuclear cells appear on the bone surface to prepare it for new osteoblasts, by removing demineralized undigested collagen, to begin bone formation and provide signals for osteoblast differentiation and migration (Florencio-silva et al. 2015), (Raggatt and Partridge 2010).

4. Formation (4 months): Mechanical stimulation and PTH signaling can promote bone formation via osteocytes that in resting conditions express sclerostin. Sclerostin binds to LRP5/6 and prevents Wnt signaling that induces bone formation. Mechanical strain on bone and PTH signaling, inhibit osteocyte expression of sclerostin. This inhibition allows Wnt signaling to work and promotes bone formation. Collagen type I is the first organic component of bone and the last is hydroxylapatite that is incorporated at the newly osteoid (Florencio-silva et al. 2015), (Raggatt and Partridge 2010).

5. Termination: Sclerostin expression increases and bone formation stops. The deposited osteoid, unmineralized organic portion of the bone matrix, is then mineralized and the bone surface returns to a resting state with bone lining cells (Raggatt and Partridge 2010).

Bone turnover markers

Bone turnover markers are biochemical products that can be measured in blood or urine and reflect the metabolic activity of bone. These molecules are extremely useful, but do not control bone metabolism, they are only indicators of the process. They can be classified as bone formation or bone resorption markers (Vasikaran et al. 2011), (Coiffier et al. 2013). Two examples of these markers are procollagen type 1 N propeptide (P1NP) and C-terminal telopeptide I (CTX-I).

P1NP is a bone formation marker. Type 1 collagen constitutes 90% of bone proteins and is initially synthetized as type 1 procollagen. This type 1 procollagen undergoes cleavage to yield amino terminal (P1NP) and C-terminal propeptide of type 1 collagen (P1CP) as represented in Fig. 5 (Samoszuk, Leuther, and Hoyle 2008).

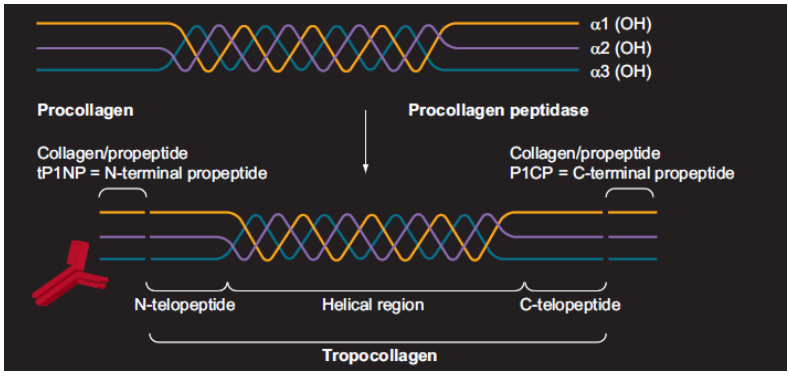

Fig. 5 – The structure of collagen type 1 found in bone (Adapted from Samoszuk et al. 2008).

CTX-I is a bone resorption marker. This molecule is released during cathepsin K activity in the bone resorption process. Osteoclasts secrete a mixture of acid and neutral proteases that degrade the collagen fibrils into fragments, including CTX. During the bone aging, the alpha form of aspartic acid present in CTX is converted to the beta form β-CTX. This last form is then released into the bloodstream during bone resorption and becomes a specific marker for the degradation of the type I collagen (Garnero, Borel, and Delmas 2001), (Delmas et al. 2000).

IL-22, IL-23 and the inflammation axis

Concerning the inflammation, IL-22, IL-23 and also IL-17A are intimately connected. All these cytokines are pro-inflammatory, meaning they promote systemic inflammation.

IL-22 is a member of the IL-10 family of cytokines. This cytokine is produced mainly by Th17, Th22 and innate lymphoid cells (ILCs) that include mucosal NK cells and the RORγt-dependent lymphoid tissue-inducer (LTi) cells. The signaling is made through a heterodimeric receptor which is composed by IL-22Rα1 and IL-10Rβ2. IL-22

is essential for the host defense against pathogens at mucosal surfaces and is also involved in wound healing. IL-10Rβ2 is ubiquitously expressed and IL-22Rα1 is expressed in liver, colon, small intestine, pancreas, kidney, skin and fibroblast like synoviocytes of joints (Rutz, Eidenschenk, and Ouyang 2013), (Yang and Zheng 2014), (Michalak-Stoma et al. 2011), (Nikoopour, Bellemore, and Singh 2014).

IL-22/IL-22Rα1/IL-10Rβ2 complex can trigger intracellular kinases such as JAK1, TYK2 and MAPK and also transcription factors, being STAT3 one of the most important (Yang and Zheng 2014). IL-22 forms dimers and binds to two IL-22Rα1 subunits and then induces phosphorylation of JAK1 and TYK2 as shown in Fig. 6, which leads to the activation of STAT3. STAT3 phosphorylation is essential in mediating the effects of IL-22 in intestinal epithelial cells (Nikoopour, Bellemore, and Singh 2014).

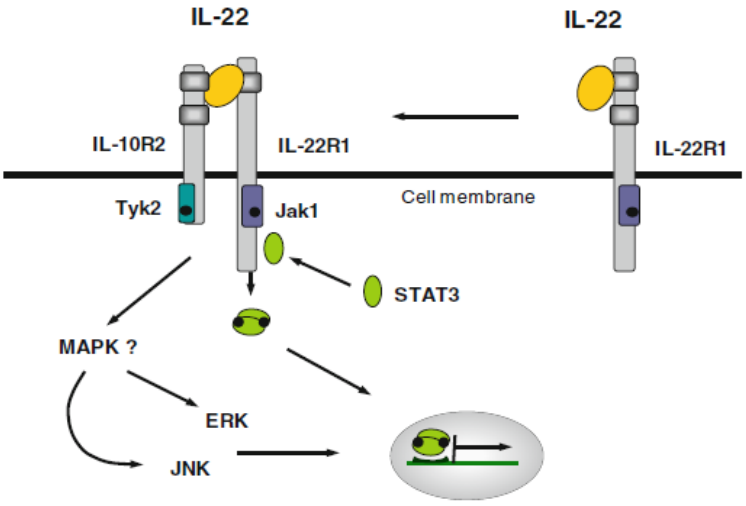

Fig. 6 – The interaction between IL-22 and IL-22 receptor complex (Adapted from Sabat et al. 2013).

When IL-22 expression becomes uncontrolled it can lead to pathology. IL-22 promotes skin inflammation when deregulated. This is particularly important in the development of psoriasis, since it is characterized by keratinocyte hyperproliferation and leukocyte infiltration and activation (Rutz, Eidenschenk, and Ouyang 2013). Its role in RA was also demonstrated as osteoclastogenic (Wolk et al. 2006), (Ikeuchi et al. 2005), (Boniface et al. 2011) and in PsA, IL-22 seems to act in the pannus formation and osteoclastogenesis in collagen induced arthritis (CIA) animal model (Geboes et al. 2009). Another study shows elevated levels of IL-22 in synovial fluid in PsA when compared with osteoarthritis (OA) patients and activated synovial T cells produced

more IL-22 than activated peripheral blood T cells in PsA (Mitra, Raychaudhuri, and Raychaudhuri 2012).

IL-23 belongs to the IL-12 family and is expressed by activated monocytes, macrophages, dendritic cells, T cells, B cells and keratinocytes. The signaling pathway is established by interaction with a heterodimeric receptor complex composed by IL-12Rβ1 and IL-23R (Fig. 7). The full signal transmission requires phosphorylation of STAT1, STAT3, STAT5 and STAT4 mainly. Increasing interaction between IL-23 and IL-23R results in the proliferation of the differentiated Th17 cells that produce IL-17A. IL-23 can also regulate pro-inflammatory cytokines. IL-23 can stimulate antigen presentation by dendritic cells (DCs) and production of interferon-γ (IFN- γ) (Michalak-Stoma et al. 2011) , (Duvallet et al. 2011), (El Hadidi et al. 2008).

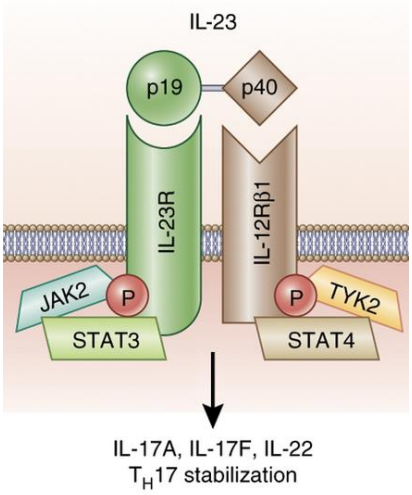

Fig. 7 – Representation of IL-23 signaling complex (Adapted from Teng et al. 2015).

When IL-23 production becomes uncontrolled it can lead to disease. IL-23 is highly related to inflammation and autoimmunity conditions. For instances IL-23 seems to play a major role in development of psoriatic plaque, thus being crucial in psoriasis (El Hadidi et al. 2008), (Michalak-Stoma et al. 2011), (Duvallet et al. 2011). It was demonstrated that PsA and Ps patients have significant elevated levels of IL-23 in serum when compared with controls (El Hadidi et al. 2008). Another study showed that mice injected intradermally with IL-23 induced a psoriasis-like phenotype (Zheng et al. 2007). Some drugs that aim to disrupt the IL-23 pathway such as ustekinumab, have showed efficacy both in Ps and PsA.

HYPOTHESIS

NSAIDs therapy alters bone resorption/formation through prostaglandin inhibition and cytokine modulation.

AIMS

1. To characterize bone metabolism parameters, cytokines and PGE_2 serum levels in PsA patients, namely before and after NSAIDs;
2. To enhance osteoclastogenesis process in an inflammatory context in PsA patients and healthy controls;
3. To assess the effect on NSAIDs in osteoclast cultures.

MATERIALS AND METHODS

Patients

In this study were included PsA patients who fulfilled the CASPAR criteria. These patients were followed at the Department of Rheumatology, Hospital de Santa Maria, Centro Hospitalar Lisboa Norte, EPE. There were no restrictions regarding treatment options namely DMARDs and biologic therapy.

Ankylosing spondylitis (AS) patients fulfilling the 1984 Modified New York Criteria, were included as a comparator group.

All patients signed an informed consent and clinical data was registered at Reuma.pt.

For control purposes a group of age and sex-matched individuals were included.

Blood samples were collected to isolate peripheral blood mononuclear cells (PBMCs) and for whole blood and serum storage.

Biomarkers and cytokines of bone metabolism

In order to quantify bone biomarkers and cytokines present in patients' and healthy controls' serum, enzyme-linked immunosorbent assays (ELISAs) were performed. All samples were preserved in -80°C until usage. The following ELISA kits were used according to the manufacturer's instructions: CTX-I and P1NP from SunRed Biological Technology, China; DKK-1, SOST, OPG and (s)RANKL from Biomedica, Austria; PGE_2 from R&D Systems Inc., USA; IL-22 and IL-23 from Raybiotech Inc., USA. All the quantifications were measured in the spectrophotometer Infinite M200 (Tecan, Switzerland).

Osteoclasts

PBMC isolation

PBMCs isolation from PsA and healthy control subjects were isolated using a density gradient centrifugation. Whole blood tubes with heparin were diluted with phosphate buffered saline 1x (PBS) and then carefully layered in Ficoll-Paque (Histopaque 1077, Sigma-Aldrich, USA). The gradients went to centrifugation at 980g during 35 minutes at room temperature (RT) in a centrifuge (Eppendorf 5810R, Germany) without acceleration or brake. The mononuclear cell layer ring was collected and washed with PBS 1x (Fig. 8). Finally the viable cells were counted in a haemocytometer using trypan blue 0.1% (Sigma-Aldrich, USA).

Fig. 8 – PBMC gradient representation. The ring represented in orange is collected and washed. After cell counting, the amount required it plated in 96 well flat bottom plates.

Cell culture

The PBMCs were cultured in Dulbecco's Modified Eagle Medium (DMEM, Biowest, France) supplemented with 5000 U penicilin/streptomicin (Invitrogen, UK), 50 mg/mL gentamicin (Invitrogen, UK), 2 mM L-Glutamin (Invitrogen, UK) and 10% fetal bovine serum (FBS, Invitrogen, UK) in 96 flat bottom plates (TPP, Sigma-Aldrich, USA). Plates were incubated in a humidified atmosphere at 37°C and 5% CO_2. Cells were plated in a density of $7.0x10^5$ cells/well. In MTT and RNA extraction timepoints at day 1, bone slices were absent, in the remaining plates for RNA extraction at day 21

and those for functional assays (TRAP staining and resorption pit assay) bone slices were added. Cells were seeded on top of bovine cortical bone slices (Immuno Diagnostic Systems Ltd, UK).

First medium exchange was performed at day 1 of culture. After this day unstimulated and stimulated conditions were created. In unstimulated condition only DMEM was added and in stimulated conditions several additions were established as represented in Fig. 9. After three days the medium was changed again and M-CSF (50 ng/mL, Peprotech, USA), sRANKL (100 ng/mL, Peprotech, USA), IL-22 (1, 10 and 50 ng/mL; Peprotech, USA) and celecoxib (1 and 10 µM, Sigma-Aldrich, USA) were added. From this time the culture medium was changed twice a week.

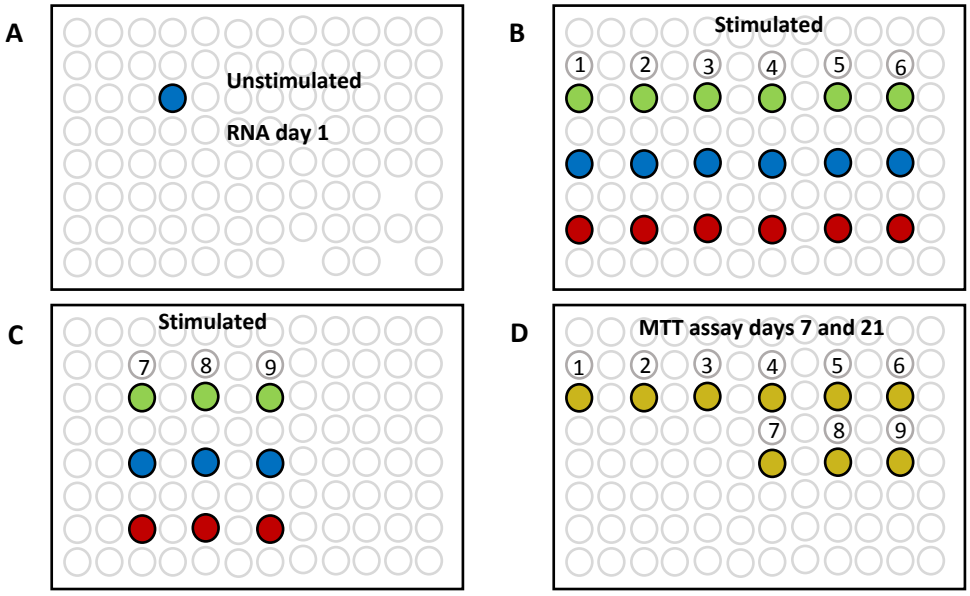

Fig. 9 – Design of 96 wells culture plates with both unstimulated and stimulated conditions. **A** Unstimulated condition, monocytes for RNA extraction at day 1 of culture. **B** Stimulated condition. 1) DMEM only, 2) DMEM+M-CSF, 3) DMEM+M-CSF+sRANKL, 4) DMEM+M-CSF+IL-22 1 ng/mL, 5) DMEM+M-CSF+IL-22 10 ng/mL, 6) DMEM+M-CSF+IL-22 50 ng/mL. **C** Stimulated condition. 7) DMEM+M-CSF+sRANKL+IL-22 1 ng/mL, 8) DMEM+M-CSF+sRANKL+IL-22 10 ng/mL, 9) DMEM+M-CSF+sRANKL+IL-22 50 ng/mL. Green, blue and red wells are for TRAP staining, RNA extraction, and resorption pit assays, respectively. **D** MTT assay performed at day 7 and 21 of culture to assess cell viability.

MTT assay

The MTT cell proliferation assay was performed to determine cells' viability during the experiment. MTT (3-(4, 5-dimethylthiazolyl-2)-2, 5-diphenyltetrazolium bromide) is a yellow reagent that is reduced by cells that are metabolically active. This results in a homogenous purple solution that can be measured by a spectrophotometer. This assay was prepared using MTT reagent (Biochemical Applichem, Germany) in a RPMI solution (Gibco, USA) at 1 mg/mL. The solution was added to the wells during 1h at 37°C. After, the plate is centrifuged at 250g for 5 minutes at RT and the supernatant is discarded. The plate is then incubated with DMSO (Merck, USA) during 10 minutes in the dark and with gentle agitation. The plate is ready for reading at 550 nm in the spectrophotometer Infinite M200 (Tecan, Switzerland).

TRAP staining

TRAP (Tartrate-resistant acid phosphatase) is an important cytochemical marker of osteoclasts. TRAP staining allows to mark and identify pre-OCs and OCs. This staining was performed using Acid Phosphate, Leucocyte Kit (TRAP, Sigma-Aldrich, USA) according to manufacturer's instructions. Initially the cells in bone slices are fixated with a fixative solution composed of paraformaldehyde 4% and then incubated with TRAP substrate during 1h at 37°C, 5% CO_2. TRAP substrate is a solution made of H_2O, sodium nitrite, fast garnet, naphtol and acetate. These components make it possible to distinguish between pre-OCs (with <3 nuclei) and mature OCs (with ≥3 nuclei). Cell's cytoplasm presents red colour in contrast to the nucleus with white colour, which remains unstained.

The number of cells was counted in the middle of the bone slices (Fig. 10) with an area of 1280x960 µm each. All the counts were made manually for each condition, using ImageJ 1.48v Software (NIH, Bethesda, MD).

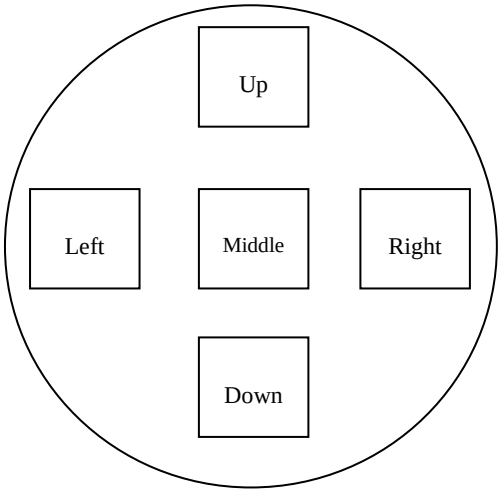

Fig. 10 – Representation of a bone slice and its orientation. Cells were counted in the middle zone.

Resorption assay

In this functional assay, bone slices were washed with PBS 1x and then incubated with 5% sodium hypochlorite for 10 minutes. Bone slices were then incubated with toluidine blue 0.1% (Sigma-Aldrich, USA) in the dark for 2 minutes. Due to this reagent, the resorption pits will become blue in colour. The measurements of the pits area was done in the middle of the bone slices (Fig. 10) with an area of 1580.25x1185.19µm each. The resorption pits' outlines were traced manually using ImageJ 1.48v Software (NIH, Bethesda, MD).

Photographs from both functional assays were taken with the brightfield microscope Leica DM2500 (Leica, Germany) under a 10x magnification objective.

Gene expression

RNA extraction and quantification

RNA was extracted from cells at days 1 and 21 from all the conditions in the OC cultures. At day 1 RNA extraction was performed using NZYol (NZYTech, Lda., Portugal) according to manufacturer's instructions. Then chloroform (VWR, USA) was added and the mixture was centrifuged. After centrifugation, the organic phase on the

top of the two phase gradient was transferred to a new tube and incubated with isopropyl alcohol (VWR, USA) in order to precipitate the RNA. After the precipitation, RNA is washed with ethanol 75% and air dried. Finally the RNA was solubilized with RNase/DNase free water (Gibco, USA). At day 21, RNA was maintained in RLT Lysis Buffer (Qiagen, Germany) before extraction with NZYol.

RNA was afterwards quantified using Nanodrop 1000 (Thermo Scientific, USA) and its concentration and purity evaluated. RNA was stored at -80°C until use.

cDNA synthesis

The complementary cDNA was synthesized at a concentration of 15 ng/µL using the DyNAmo™ cDNA Synthesis Kit (Thermo Scientific, USA), according to manufacturer's instructions. The synthesis was performed using reverse transcriptase M-MuLV RNase H^+ and random hexamers. The PCR elongation phase started at 37°C during 30 minutes and the termination phase took place at 85°C during 5 minutes to inactivate the reverse transcriptase. cDNA was stored at 4°C.

qPCR and gene expression quantification

Quantitative PCR was used in this study in order to quantify osteoclast gene expression. The genes selected to study OCs were CTSK, RANK, CSF1R, NFATc1 and ribosomal RNA 18S as housekeeping gene. Primers were designed using the primer-BLAST (Ye et al. 2012) software and having into consideration the amplicon size of less than 100 bp, 60°C annealing temperature and the exon-exon junction. Primer sequences and characteristics can be found in Table II in ANNEX I.

The DyNAmo™ Flash SYBR Green qPCR Kit (Thermo Scientific, USA) was used according to the manufacturer's instructions. SYBR Green binds to the double stranded amplified product of qPCR and emits fluorescence, which is then detected by the thermocycler's detector (7500 Fast, Applied Biosystems, USA). 15 ng/µL of cDNA were used for RT-PCR. The protocol begins with an initial denaturation at 95°C during 10 minutes in order to activate the hot start DNA polymerase and also to denature the template cDNA. Then a short denaturation step takes place during 15 seconds at the

same temperature. This last step is followed by a combined annealing/extension step at 60°C during 60 seconds, for 50 cycles. The final step is the melting curve, which allows the strands to denature in a gradual process. This step permits the curve validation. In order to analyze the results the 7500 Software v2.0.6 (Applied Biosystems, USA) was used.

The efficiency and results of the qPCR were analyzed using the standard curve method. To make the standard curves, cDNA templates from RNA trabecular bone from individuals with normal bone mineral density (BMD) and without clinical risk factors for osteoporosis or other bone related diseases were used. The initial cDNA quantity was 30 ng/mL and then serial 1:3 dilutions, down to 0.37 ng/mL, were made for the standard curve. The cycle threshold (Ct) is defined as the number of cycles required for the fluorescent signal to cross the threshold and exceed the background level. The efficiency of the qPCR should be 100%, which means that for each cycle the amount of product doubles. A good reaction should vary between 90-100% in efficiency, which corresponds to a slope between -3.58 and -3.10. The conversion of the Ct value in relative expression levels is performed with the slope and the Y intersect extracted from the standard curve and applying the equation $10^{(\text{Ct-Y intersect})/\text{slope}}$ (Wong and Medrano 2005). The values obtained should then be normalized with the housekeeping gene 18S rRNA.

Statistical analysis

Statistical analysis was performed using GraphPad Prism 5 Software (GraphPad Software, Inc., USA). Data is represented as median [interquartile range]. According to normality test distribution, for two variable comparison t-test or Mann-Whitney test were used. For paired variables Wilcoxon matched pairs test or paired t test, depending on the normality test distribution, were used as well. For more than two variables Kruskall-Wallis test was used with Dunn's post hoc test. Categorical variables are expressed as relative frequencies and for them, Chi-Square test was used. *P* values lower than 0.05 were considered statistically significant.

Other methods

Osteoblasts

The MG-63 cell line (Faculdade de Medicina Dentária do Porto, Portugal) was cultured in α-MEM (Gibco, USA) supplemented with 5000 U penicilin/streptomicin (Invitrogen, UK), 2.5 µg/mL amphotericin B (Sigma-Aldrich, USA) and 10% FBS (Invitrogen, UK) at 37°C, 5% CO_2, for expansion.

For differentiation, cells were cultured in α-MEM (Gibco, USA) supplemented with 5000 U penicilin/streptomicin (Invitrogen, UK), 2.5 µg/mL amphotericin B (Sigma-Aldrich, USA), 50 µg/mL vitamin C (Fluka analytical, USA), 0.1 M β-glicerolphosphate (Fluka analytical, USA), 2 mM L-Glutamin (Invitrogen, UK) and 10% FBS (Invitrogen, UK) at 37°C, 5% CO_2. Medium was changed every three days.

The hFOB 1.19 cell line (ATCC, USA) was cultured in DMEM:F12 (1:1) (Gibco, USA) supplemented with 5000 U penicilin/streptomicin (Invitrogen, UK), 0.3 mg/mL G418 (Biowest, France), 15 mM HEPES (Biowest, France) and 10% FBS (Invitrogen, UK) at 33.5°C, 5% CO_2, for expansion.

Animal mouse model of spondyloarthritis

In parallel to the work developed in the study of PsA patients, which constitutes the main body of this thesis, further experience was acquired integrated in a complementary project studying membrane bound TNF (mTNF) mice, an animal model of spondyloarthritis.

mTNF mice is a transgenic line which expresses a mouse TNF gene. This gene contains a deletion of the codons enconding the 1st to the 12th aminoacids of the mature 17-kDa TNF protein. mTNF mice develop spontaneously peripheral arthritis and spondylitis. They have a SpA-like phenotype with axial and peripheral joint involvement. The arthritis penetrance is 100%, which is a major advantage in this model. Arthritis is characterized in this model by deformation of the joints and loss of grip and spondylitis by crinkled tails and hunchback formation. These symptoms start at

4-6 weeks of age and become more severe over time. However they do not lose weight and can survive more than 8 months (van Duivenvoorde, Leonie M., van Tok, Melissa N., Baeten 2013).

Colony establishment and maintenance

mTNF mice are a heterozygous strain and for that reason breedings are done with C57BL/6J wild-type (WT) mice. The heterozygous animals came from Amsterdam Medical Center, University of Amsterdam. After the arrival breeding pairs were made, 2 females and 1 male per cage. The colony was not easy to establish, the animals were already 14 weeks old with visible phenotype. The first pups were born 7 weeks later. When these young animals became adults and able to reproduce, the first attempt to rederive the strain to a cleaner room, specific pathogen free (SPF), was made. It is known that the environment plays a crucial role in the microbiota of the animals and therefore can alter the way the disease is expressed. In a cleaner room, the animals should present the symptoms later. In order to maintain the strain for long term, rederivation is necessary, beyond the environment issues.

Many rederivations were done until a successful pregnancy was detected. Before the birth, the female selected for rederivation is subjected to a caesarean by the veterinary of the rodent facility. The pups are then put into a new cage with a foster mother, who had pups recently and can take care of these new ones.

Actually mTNF mice are in two distinct rooms: SPF room and quarantine room. In the SFP room the animals are still in breeding to establish a colony there. In quarantine room, a breeding trio is maintaining the colony with success.

Genotyping

As a heterozygous strain, all the pups resulting from the breedings should be genotyped. A piece of ear is taken for mice identification in the rodent facility and is harnessed as DNA sample. These pieces are then placed in a mixture of 100 µL of lysis buffer (Viagen, USA) and 1 µL of proteinase K (1 mg/mL; Sigma-Aldrich, USA) and incubated overnight at 55°C. Then the temperature is set to 85°C to inactivate proteinase K. These steps are followed by the PCR amplification and then the electrophoresis gel (see ANNEX II for protocol).

Monitoring

Each animal is monitored once a week. The monitoring is made after the weaning and mice genotyping and consists in weight measurement, paw score and annotations of observations considered relevant, like pregnancies and first symptoms appearance. All animals are photographed with emphasis in tail and paws.

The paw score is a 5 point score (0-4). According to the European Guidelines for Animal Experimentation, this score is based on increasing levels of swelling and periarticular erythema. The maximum score is defined as the sum of the scores for all the paws 16 (4+4+4+4):

0 - Normal
1 – Erythema and swelling of one ankle
2 – Erythema and swelling of one ankle and proximal half of tarsal joints
3 – Erythema and swelling of one ankle and all tarsal joints up to metatarsal joints
4 – Erythema and swelling of one entire paw, including digits

Euthanasia

Mice euthanasia was done by CO_2. After euthanasia, cardiac puncture was performed. The whole blood from the mice were incubated during 1h at 37°C in dry bath and then centrifuged to obtain serum for protein quantifications.

Necropsy

During the necropsy, front and hind paws were collected as well as L3/L4 and L5 vertebrae, cervical vertebrae that were damaged due to the hunchback, left and right tibias, left and right femurs and tail vertebrae that were crinkled. Considering the internal organs: large and small intestine portions, small intestine transition and cecum, spleen and liver were also collected.

For histology analysis in paraffin embedding organs were stored in cassettes and then in a container with formalin 10% during 5 days. Bone was decalcified with EDTA 10%, pH = 7.0, for 2 weeks. After, the tissue is processed which includes dehydration, clearing (replacing the dehydrant with a substance that will be miscible with the paraffin) and impregnation (the tissue is embedding in paraffin blocks). Then the blocks are ready to cut in the microtome.

Tissues were also stored in OCT (cryoprotective embedding medium), snap frozen (directly into liquid nitrogen) and in ethanol 70%.

H&E staining

Hematoxylin and eosin staining has 3 steps:

1 – Deparaffinization and hydration: slides are immersed in xylene during 15 minutes, following by 10 minutes in 100% ethanol. Then slides are immersed in 95% ethanol for 10 minutes and then in 70% ethanol during 10 minutes. The last step is immersing the slides in distilled water for 5 minutes.

2 – Staining: Hematoxylin is added to the slides (200 µL) and incubated during 5 minutes. After the incubation, slides are washed in running water in reverse position. Then the slides are incubated in distilled water during 5 minutes. Eosin is added (400µL) and incubated during 30 seconds. The slides are washed in running water in reverse position and then incubated during 5 minutes in distilled water.

3 – Dehydration: the same steps as hydration but in inverse order. First comes 70% ethanol during 30 seconds, then 95% ethanol during 30 seconds as well, next step is 100% ethanol for 30 seconds and last step is xylene during 15 minutes. After this the slides are mounted and left to dry.

Immunohistochemistry (IHC)

Before performing IHC to different animals, it is necessary to optimize protocols for inflammatory cells and bone markers. Optimizations were done to the following antibodies: CD3 (T cells marker), CD19 (B cell marker), CD68 (monocytes/macrophages marker), CD163 (monocytes/macrophages marker) and SOST (osteocyte marker).

Generally all IHC protocols have a deparaffinization step, followed by antigenic retrieval (sometimes optional), then endogenous peroxidase blocking and total protein blocking. These blockings are essential to reduce the background in the staining. The next step is the addition of the primary antibody and washes with PBS/Triton. Then the secondary antibody is added, Horse Radish Peroxidase (HRP) and it is followed by washes with PBS/Triton. The developing solution, 3,3′-Diaminobenzidine (DAB) is added and then the slides are washed with distilled water. After, hematoxylin contrast is done and finally the last step, dehydration is performed (see ANNEX III for detailed protocol example).

RESULTS

I. ELISAs: protein quantifications in serum

Patient characteristics

This study included 26 patients diagnosed with PsA, 16 men and 10 women. The median age of the patients was 48.5 [34-60] years and the median of symptoms duration was 2.5 [0.81-5] years, as shown in Table I.1. From these 26 patients, 12 of them were followed after NSAID therapy. Six AS patients were also recruited as disease comparators, 3 men and 3 women with a median age of 42 [31.75-49] years and a median of symptoms of 13.5 [5-26.5] years. Twenty three healthy age and gender matched subjects were included as controls as well, 10 men and 13 women with a median age of 45 [35-52] years.

The majority of PsA patients, has peripheral disease (79%) but in a high percentage also axial and entheseal involvement as shown in Table I.1. In AS patients axial involvement was predominant and some peripheral involvement was detected. Concerning HLA-B27, only 16% of PsA patients are positive in contrast with 50% of AS patients.

Table I.1 – Demographic and clinical data of PsA and AS patients.

	Healthy	PsA patients	AS patients	*p* value
N	23	26	6	
Age (years)	45 [35-52]	48.5 [34-60]	42 [31.75-49]	0.4480
Male (%)	57%	62%	50%	0.6085
Symptoms duration (years)	NA	2.5 [0.81-5]	13.50 [5-26.5]	0.0323
Axial involvement (% yes)	NA	57%	75%	0.3878
Peripheral involvement (% yes)	NA	79%	25%	0.042
Entheseal involvement (% yes)	NA	64%	0%	
HLA-B27 (% positive)	NA	16%	50%	0.0845
NSAIDs (% yes)	NA	0%	50%	
NSAIDs duration (months)	NA	0	3 [3-58]	
DMARDs (% yes)	NA	11.1%	0%	
Bisphosphonates (% yes)	NA	0%	0%	
Anti-TNF (% yes)	NA	0%	33%	
ESR (mm/h)	NA	16 [8-37]	20.5 [13.5-36.5]	0.2722
CRP (mg/L)	NA	5 [1.08-11.75]	4.15 [2.15-7.6]	0.8275

Results are expressed in median [interquartile range 25-75]. *p* values lower than 0.05 are considered statistically significant. PsA – psoriatic arthritis; AS – ankylosing spondylitis; NA – not applicable; NSAIDs – non-steroidal anti-inflammatory drugs; DMARDs – disease-modifying anti-rheumatic drugs; ESR – erythrocyte sedimentation rate; CRP – C-reactive protein.

From this group of patients, only AS was previously treated with NSAIDs (50%) and anti-TNF therapy (33%) and a small percentage (11.1%) of PsA was under DMARDs. None of the patients was under bisphosphonates. Inflammatory markers, ESR and CRP, were both increased in the two diseases and when compared, the values are similar (Table I.1).

Considering the 12 paired PsA patients, 6 men and 6 women, the median age is 35 [29-53.5] years with a median symptoms duration of 3 [1.75-5.5] years, as shown in Table I.2. Almost half of the patients is positive for HLA-B27 (43%) and axial, peripheral and entheseal involvements is present in the majority of the subjects (more than 50%) just like before (Table I.1 and Table I.2)

Table I.2 – Demographic and clinical data of paired PsA patients.

	Healthy	Paired PsA patients		
N	12	12		
Age (years)	35.5 [33.25-43.75]	35 [29-53.5]		
Male (%)	58.3%	50%		
Symptoms duration (years)	NA	3 [1.75-5.5]		
Axial involvement (% yes)	NA	50%		
Peripheral involvement (% yes)	NA	60%		
Entheseal involvement (% yes)	NA	75%		
HLA-B27 (% positive)	NA	43%		
NSAIDs (% yes)	NA	100% (after)		
NSAIDs duration (months)	NA	7 [3-9.75]		
DMARDs (% yes)	NA	8%		
Bisphosphonates (% yes)	NA	0%		
Anti-TNF (% yes)	NA	0%		
		NSAID Therapy		
		Before	After	*p* value
ESR (mm/h)	NA	15.5 [10-33]	13 [8-29.5]	0.8587
CRP (mg/L)	NA	5 [0.63-9.58]	4.6 [0.55-12.05]	0.9735

Results are expressed in median [interquartile range 25-75]. *p* values lower than 0.05 are considered statistically significant. PsA – psoriatic arthritis; NA – not applicable; NSAIDs – non-steroidal anti-inflammatory drugs; DMARDs – disease-modifying anti-rheumatic drugs; ESR – erythrocyte sedimentation rate; CRP – C-reactive protein.

NSAID therapy was present in all patients (100% in Table I.2) only in the follow up. After the beginning of the therapy the median duration was 7 [3-9.75] months. Only 8% of the subjects were under DMARDs and none was under bisphosphonates or anti-TNF therapies.

Inflammatory markers, ESR and CRP, seem to have slightly decreased after NSAID therapy but the *p* value is almost 1, indicating that the results are similar between before and after.

Inflammatory cytokines and biomarkers of bone metabolism

In order to understand better the activation of bone metabolism pathways in PsA patients, different biomarkers of bone turnover, bone remodeling, Wnt pathway and pro-inflammatory cytokines were determined.

Bone turnover markers, CTX-I and P1NP were measured in the patients' serum. CTX-I levels are significantly higher in healthy controls in comparison with PsA patients (p=0.0282) as can be seen in Fig. 11. P1NP levels were higher in AS patients (p=0.0162), when comparing with controls and PsA subjects (Fig. 11). When comparing

the ratio between CTX-I and P1NP, the levels are decreased in patients with significant *p* values.

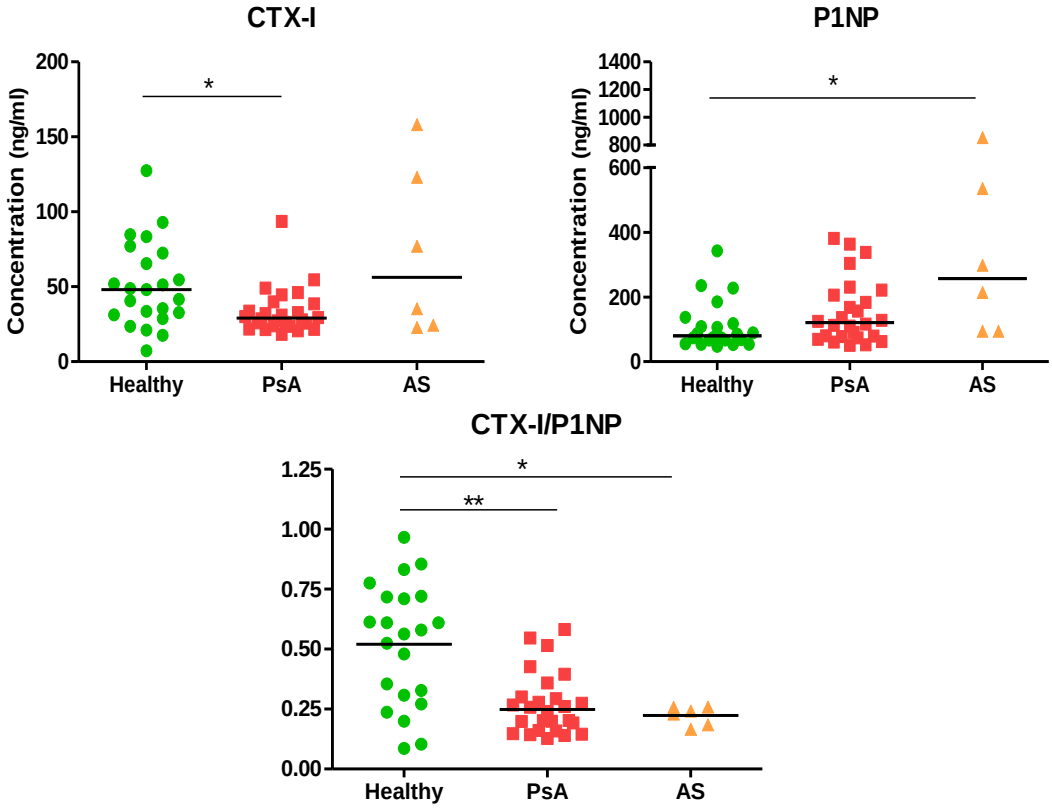

Fig. 11 – Serum levels of CTX-I, P1NP and CTX-I/P1NP ratio of PsA and AS patients. Bars represent median values. Results were analyzed with Kruskal-Wallis test. *p* values lower than 0.05 are considered statistically significant. *p<0.05, **p<0.01. CTX-I – C-terminal telopeptide I; P1NP – Procollagen type 1 N propeptide.

sRANKL levels are very similar between groups, OPG levels are increased in PsA in comparison with controls (p=0.0195) as seen in Fig. 12. The sRANKL/OPG ratio seems to be lower in patients than in controls and there is a significant difference between PsA and AS patients (p=0.0357), PsA have lower levels than AS.

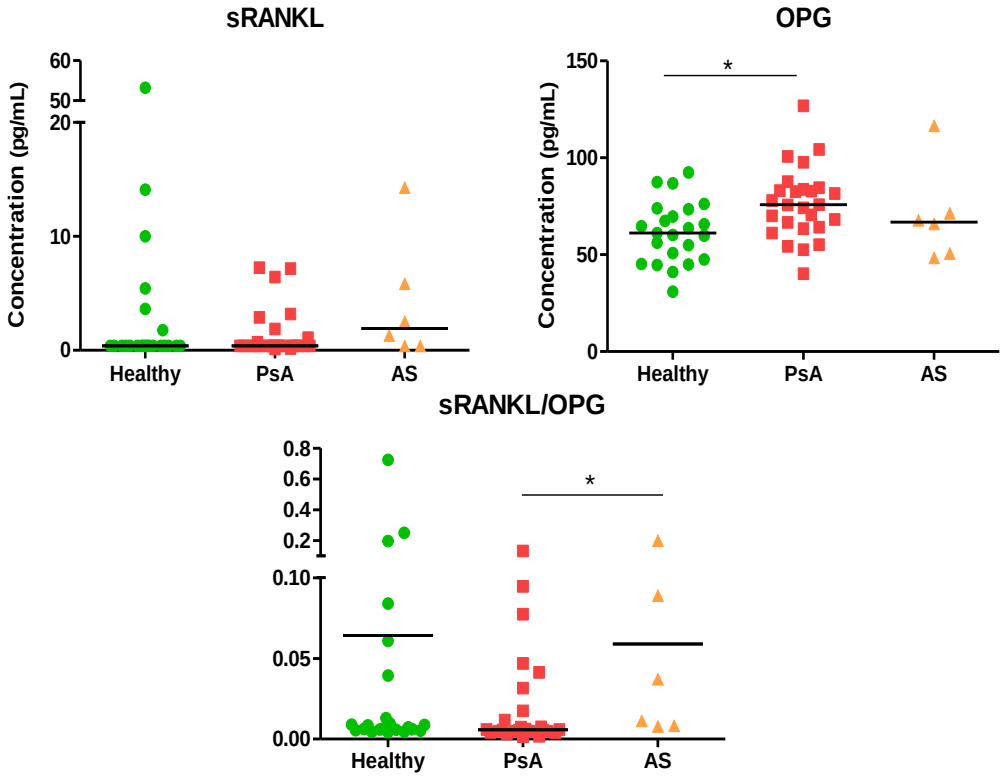

Fig. 12 – Serum levels of sRANKL, OPG and sRANKL/OPG ratio of PsA and AS patients. Bars represent median values. Results were analyzed with Kruskal-Wallis test. *p* values lower than 0.05 are considered statistically significant. *p<0.05. sRANKL – soluble receptor activator of nuclear factor kappa-B ligand; OPG – osteoprotegerin.

In terms of the Wnt pathway inhibitors, DKK-1 and SOST, DKK-1 levels show a trend to be lower in controls but the difference was not statistically significant. SOST levels are significantly decreased in both patients' groups (p<0.0001) as shown in Fig.13.

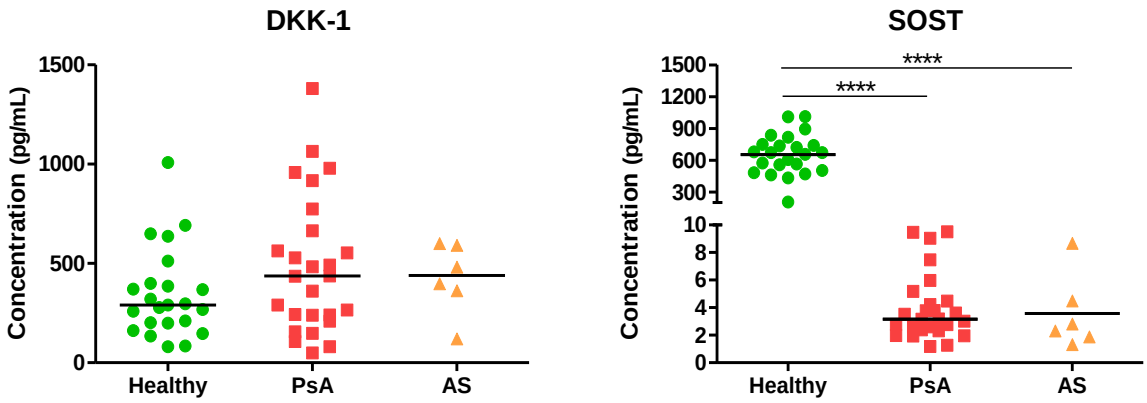

Fig. 13 - Serum levels of DKK-1 and SOST of PsA and AS patients. Bars represent median values. Results were analyzed with Kruskal-Wallis test. *p* values lower than 0.05 are considered statistically significant. ****p<0.0001. DKK-1 – dickkopf-related protein 1; SOST – sclerostin.

Pro-inflammatory cytokines, IL-22 and IL-23 were also evaluated. IL-22 levels seem to be lower in patients but this difference was not statistically significant. IL-23 level distribution is very similar in each group. PGE_2 tend to be decreased in patients, comparing to controls but once again there is no significance. Healthy controls in this group are only 12, the same 12 used for paired PsA samples comparisons. The demographic characteristics can be found in Table I in ANNEX IV.

When comparing paired PsA before and after NSAID therapy, there is no statistical significance in any of the assessed parameters. CTX-I and P1NP levels in paired PsA samples are very similar, but CTX-I control levels are higher than PsA, as observed in the general population of this study and P1NP are lower (Fig. 15). The ratio CTX/P1NP in healthy controls is also increased when comparing with patients.

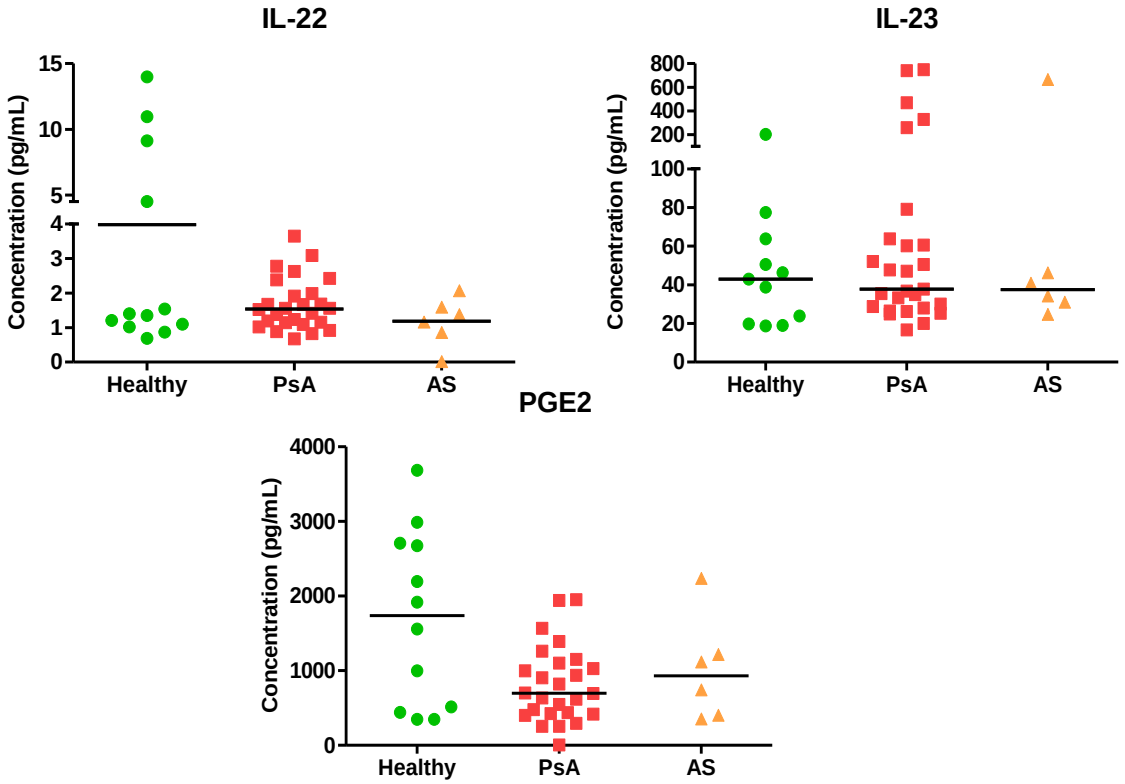

Fig. 14 - Serum levels of IL-22, IL-23 and PGE_2 of PsA and AS patients. Bars represent median values. Results were analyzed with Kruskal-Wallis test. *p* values lower than 0.05 are considered statistically significant. IL – interleukin; PGE_2 – prostaglandin E2.

sRANKL and OPG levels, before and after NSAID therapy, are constant and when comparing with controls the values do not vary, as shown in Fig. 16. The sRANKL/OPG ratio do not display any statistical significance.

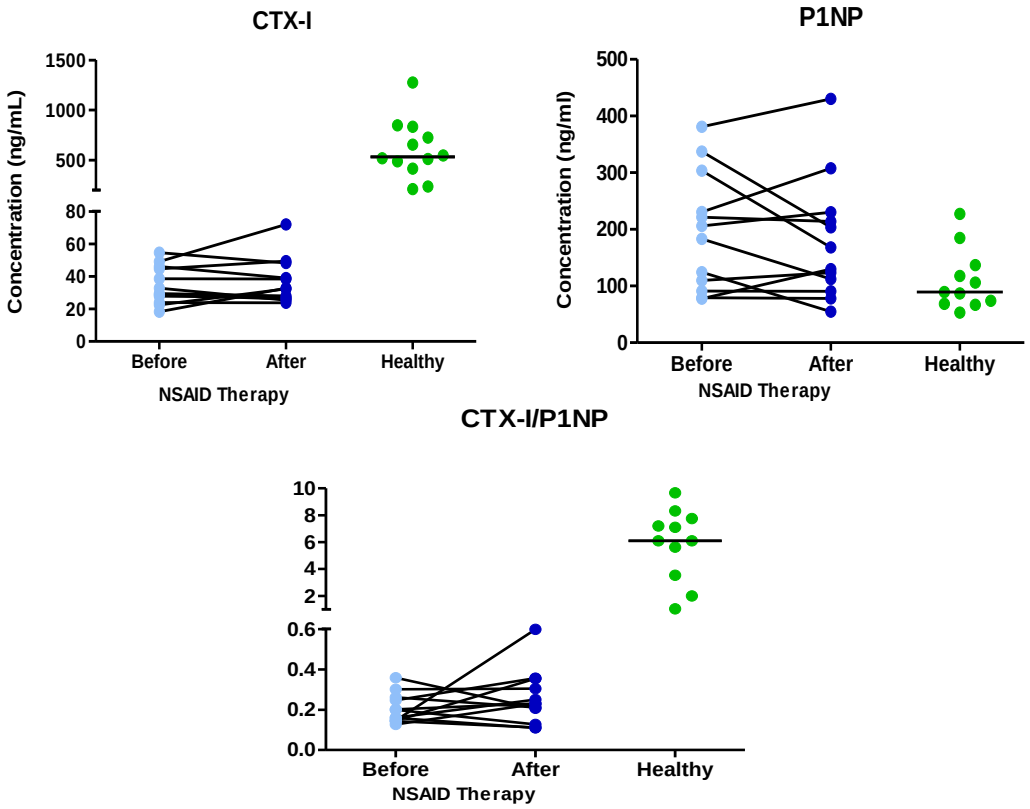

Fig. 15 – Serum levels of CTX-I, P1NP and CTX-I/P1NP ratio of paired PsA patients before and after NSAID therapy. Bars represent median values. Results were analyzed with Wilcoxon matched pairs test. *p* values lower than 0.05 are considered statistically significant. sRANKL – soluble receptor activator of NF-kB; OPG – osteoprotegerin; NSAID – non-steroidal anti-inflammatory drug.

Regarding Wnt pathway inhibitors, DKK-1 and SOST levels before and after NSAID therapy are not statistically significant. DKK-1 levels do not differ with significance from controls. SOST levels seem to be increased in healthy controls in comparison with patients (Fig. 17).

Pro-inflammatory cytokines, IL-22 and IL-23 also have similar levels of protein quantification before and after NSAID therapy. Controls in both cytokines have a disperse pattern with no statistical significance (Fig. 18). PGE_2 levels seem to be the same or higher after therapy and healthy controls also have a disperse pattern.

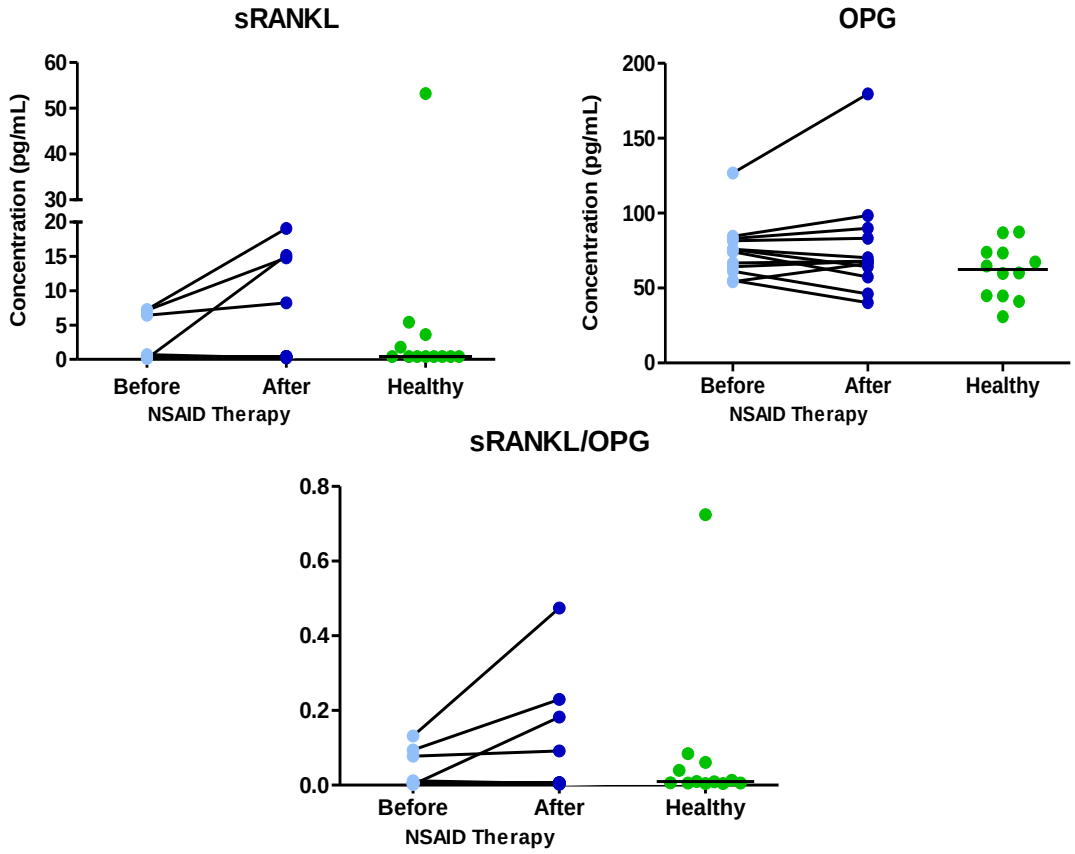

Fig. 16 - Serum levels of sRANKL, OPG and sRANKL/OPG ratio of paired PsA patients before and after NSAID therapy. Bars represent median values. Results were analyzed with Wilcoxon matched pairs test. *p* values lower than 0.05 are considered statistically significant. sRANKL – soluble receptor activator of nuclear factor kappa-B ligand; OPG – osteoprotegerin; NSAID – non-steroidal anti-inflammatory drug.

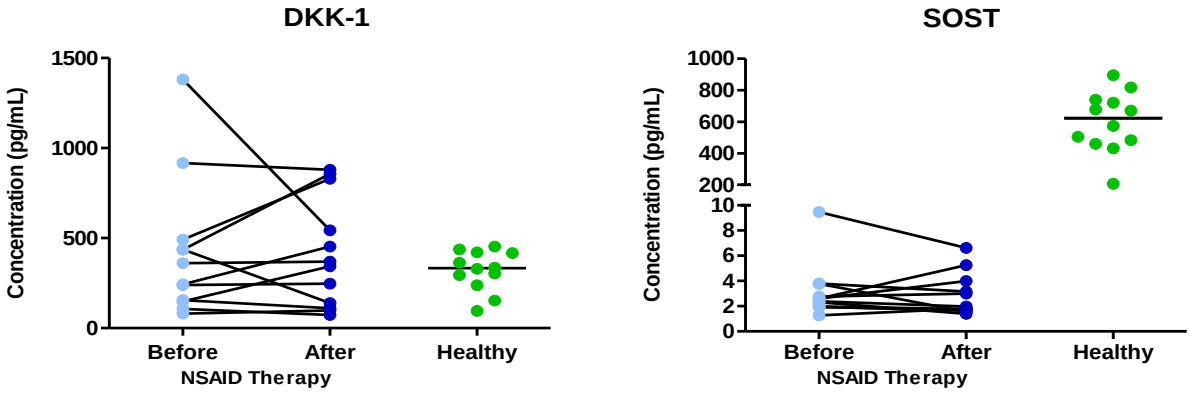

Fig. 17 – Serum levels of DKK-1 and SOST of paired PsA patients before and after NSAID therapy. Bars represent median values. Results were analyzed with Wilcoxon matched pairs test. *p* values lower than 0.05 are considered statistically significant. DKK-1 – dickkopf-related protein 1; SOST – sclerostin; NSAID – non-steroidal anti-inflammatory drug.

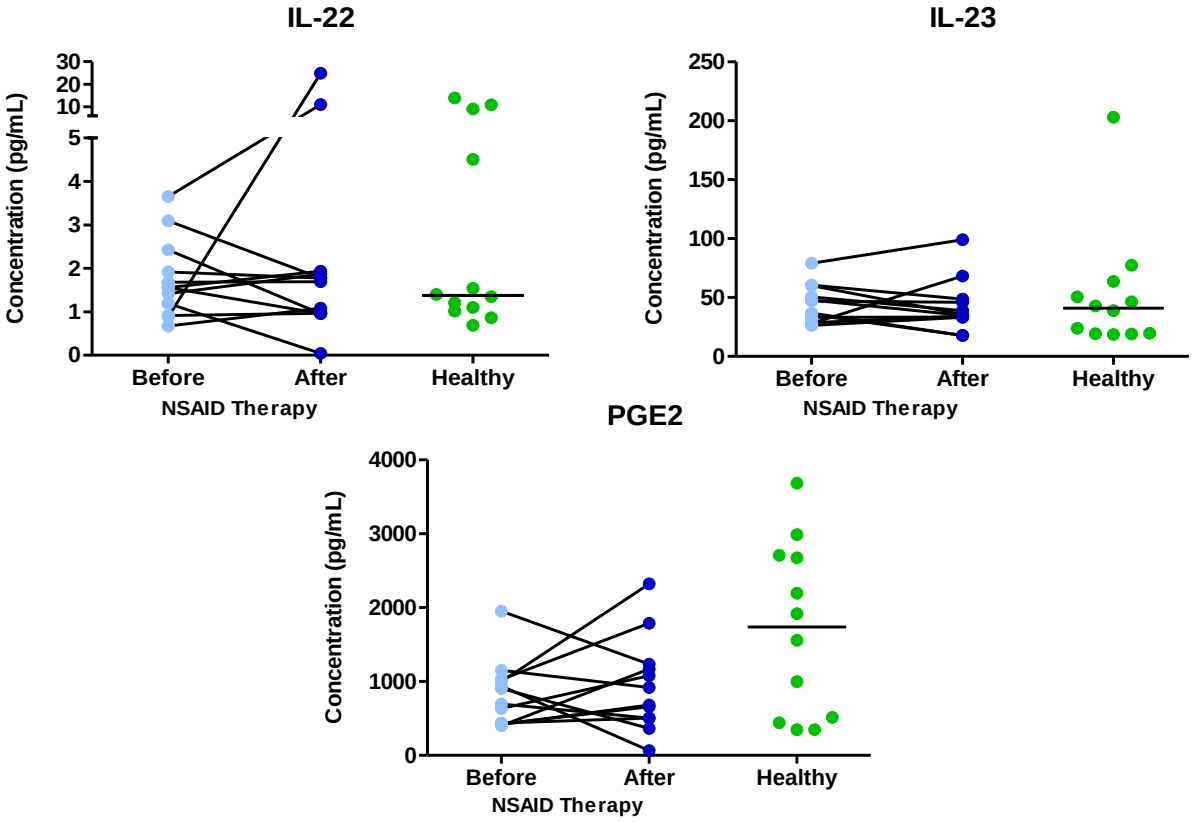

Fig. 18 - Serum levels of IL-22, IL23 and PGE_2 of paired PsA patients before and after NSAID therapy. Bars represent median values. Results were analyzed with Wilcoxon matched pairs test. *p* values lower than 0.05 are considered statistically significant. IL – interleukin; PGE_2 – prostaglandin E2; NSAID – non-steroidal anti-inflammatory drug.

II. Osteoclast assays

This study was divided in two steps: IL-22 concentration optimization and celecoxib stimulation.

Sample characteristics

For the IL-22 part, the study included 4 healthy subjects, 2 men and 2 women. The median age of the subjects was 42 [37-49.25]. For the celecoxib part, the study included 3 healthy subjects, 2 men and 1 woman, and 2 PsA patients, 1 man and 1 woman. The median age of the controls was 39 [28-42] and the median age of patients was 39 [38-40]. PsA patients were not having any kind of therapy.

Pre-osteoclast, osteoclast and pit counts

After PBMC isolation, cells were cultured in different conditions and at each timepoint *ex vivo* functional assays were performed in unstimulated and stimulated conditions at day 21 (Table II.1). Under these circumstances it is expected to see mature OCs and bone resorption at day 21 in stimulated conditions (Holloway et al. 2002).

Table II.1 – Osteoclast cell culture conditions: unstimulated and stimulated.

OSTEOCLAST CELL CULTURE CONDITIONS *IN VITRO*	
Unstimulated	**Stimulated**
Mono (monocytes)	M-CSF + RANKL
M-CSF	IL-22 1 ng/mL + M-CSF
	IL-22 10 ng/mL + M-CSF
	IL-22 50 ng/mL + M-CSF
	IL-22 1 ng/mL + M-CSF + RANKL
	IL-22 10 ng/mL + M-CSF + RANKL
	IL-22 50 ng/mL + M-CSF + RANKL
	Celecoxib 1 ng/mL + M-CSF
	Celecoxib 10 ng/mL + M-CSF
	Celecoxib 1 ng/mL + IL-22 (10 ng/mL) + M-CSF + RANKL
	Celecoxib 10 ng/mL + IL-22 (10 ng/mL) + M-CSF + RANKL
M-CSF concentration was always 50 ng/mL and RANKL concentration 100 ng/mL	

TRAP staining turns the cell cytoplasm reddish and allows to count the nuclei, since they remain white, unstained. In Fig. 19 it is possible to observe a representative image of pre-OC and OC counting. Pre-OCs are defined as cells with less than 3 nuclei and OCs with 3 or more nuclei.

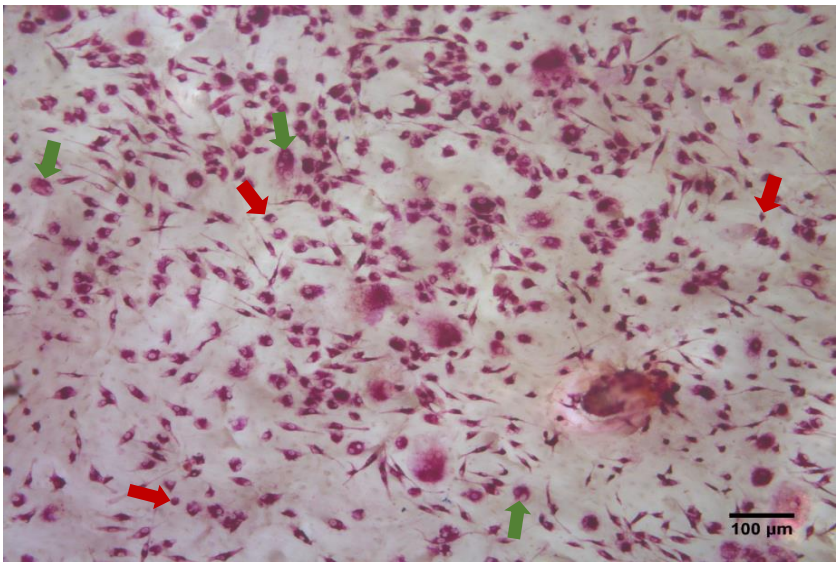

Fig. 19 – Representative image of pre-OCs (red arrows) and OCs (green arrows) with TRAP staining. Scale bar corresponds to 100 µm.

In resorption assays, pits are acidic structures with purple/blue appearance after being incubated with toluidine blue. In Fig. 20 is shown a representative image of resorption pits in a stimulated condition.

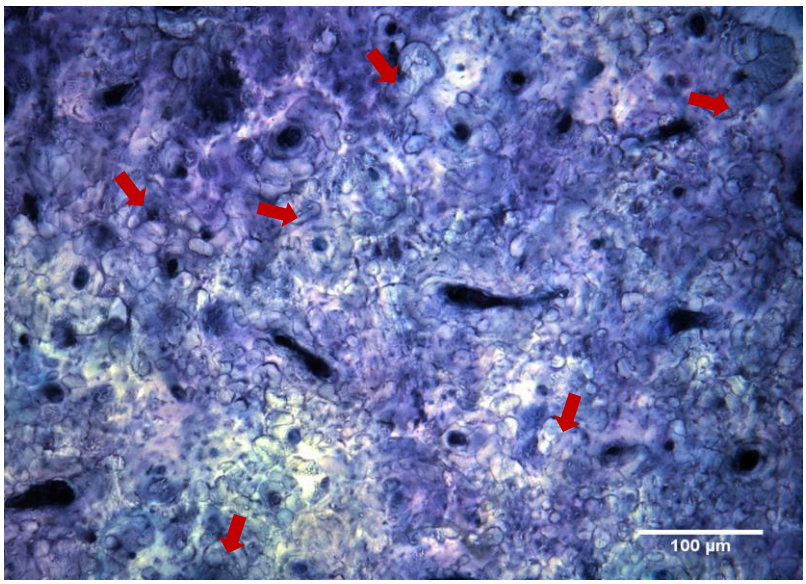

Fig. 20 – Representative image of resorption pits (red arrows) with toluidine blue staining. Scale bar corresponds to 100 µm.

Without stimuli, cells should not develop mature osteoclasts neither resorption pits. Cells in the presence of a stimuli for osteoclastogenesis will develop osteoclasts and these osteoclasts will resorb bone. In Fig. 21 is visible the difference between unstimulated conditions (Mono and M-CSF) and a stimulated condition (M-CSF+RANKL).

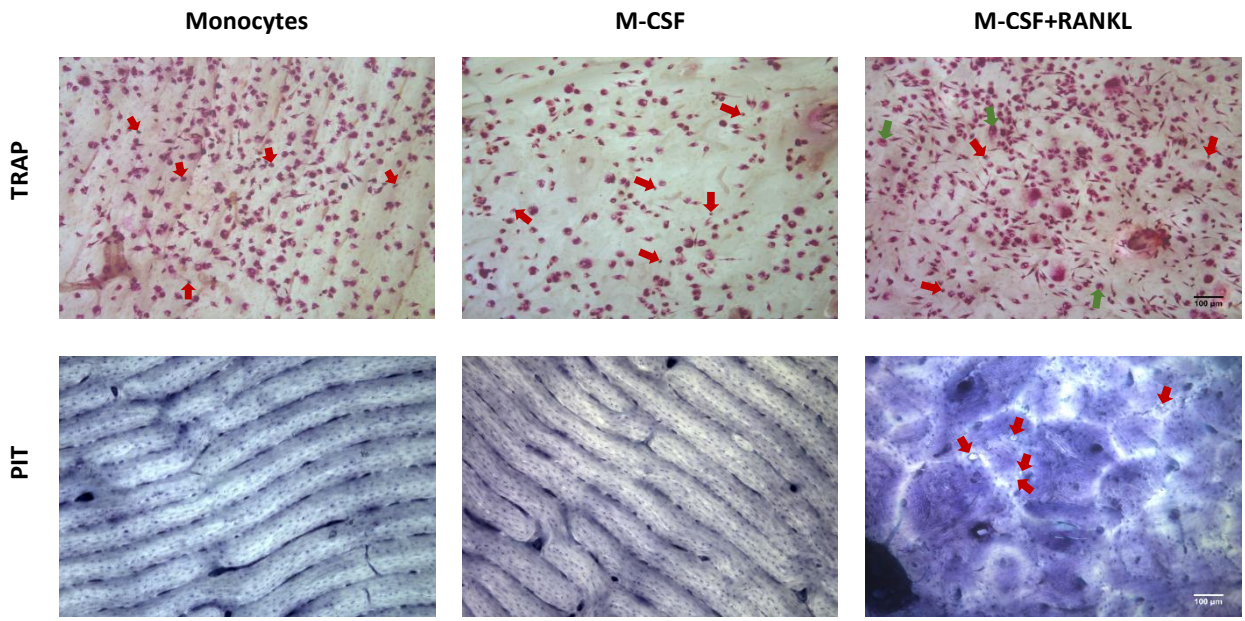

Fig. 21 – Pre-OCs (red arrows in TRAP staining), OCs (green arrows) and resorption pits (red arrows in toluidine blue staining) under stimulated and unstimulated conditions at day 21. Scale bar corresponds to 100 µm.

In the IL-22 concentration optimization part, the number of pre-OC, OC and nuclei per OC was counted. In pre-OC number there is an increase in IL-22 at 1 ng/mL, in IL-22 at 50 ng/mL and in IL-22 at 10 ng/mL with and without RANKL, when comparing to positive control M-CSF and RANKL. All conditions had higher number of pre-OC than mono condition (Fig. 22). OC number is higher in M-CSF than in all the other conditions, followed by IL-22 at 10 ng/mL. Nuclei number per OC have a similar pattern in all conditions as shown in Fig. 22.

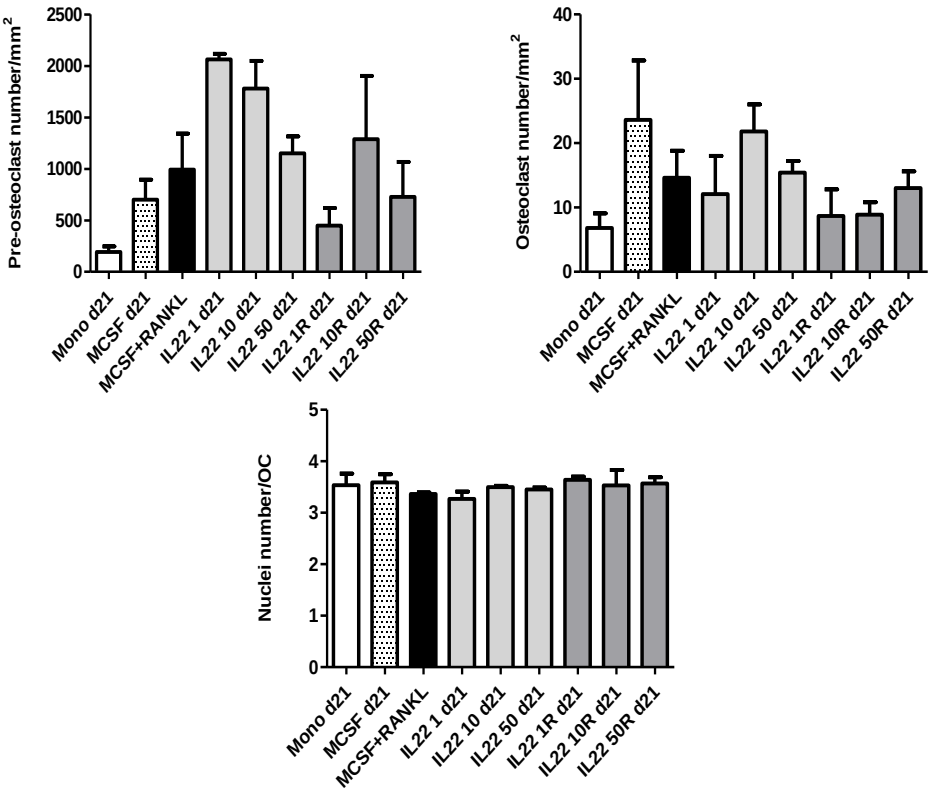

Fig. 22 – IL-22 optimization. Number of pre-OC, OC and nuclei per OC under unstimulated and stimulated conditions. Median values are shown with 75% percentile. Results were analyzed with Wilcoxon matched pairs test. *p* values lower than 0.05 are considered statistically significant. Mono – monocytes; M-CSF – macrophage colony-stimulating factor; RANKL – receptor activator of nuclear factor kappa-B ligand; IL – interleukin; IL22 1 – IL-22 at 1 ng/mL; IL22 10 – IL-22 at 10 ng/mL; IL22 50 – IL-22 at 50 ng/mL. IL22 1R – IL-22 at 1 ng/mL with RANKL; IL22 10R – IL-22 at 10 ng/mL with RANKL; IL22 50R – IL-22 at 50 ng/mL with RANKL; d21 – day 21.

In terms of resorption pits, pit number and pit number per OC were also measured. Pits were only observed in positive control M-CSF and RANKL and in IL-22 with RANKL. Pit number seems to be higher in IL-22 at 1 ng/mL with RANKL and the other values are very similar as seen in Fig. 23. However neither of this values is statistically significant.

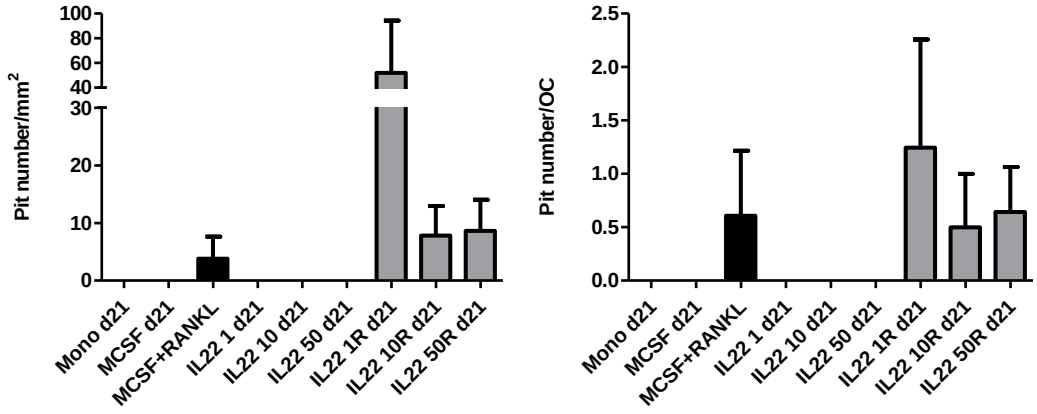

Fig. 23 – IL-22 optimization. Pit number and pit number per OC under unstimulated and stimulated conditions. Median values are shown with 75% percentile. Results were analyzed with Wilcoxon matched pairs test. *p* values lower than 0.05 are considered statistically significant. Mono – monocytes; M-CSF – macrophage colony-stimulating factor; RANKL – receptor activator of nuclear factor kappa-B ligand; IL – interleukin; IL22 1 – IL-22 at 1 ng/mL; IL22 10 – IL-22 at 10 ng/mL; IL22 50 – IL-22 at 50 ng/mL. IL22 1R – IL-22 at 1 ng/mL with RANKL; IL22 10R – IL-22 at 10 ng/mL with RANKL; IL22 50R – IL-22 at 50 ng/mL with RANKL; d21 – day 21.

Not only were the number of pits measured but also the percentage of area that they resorbed. The percentage of resorbed area is higher in IL-22 at 1 ng/mL with RANKL, when comparing with the other conditions. The reabsorbed area per pit is higher in that condition as well, followed by IL-22 with RANKL at concentrations 10 and 50 ng/mL with very similar values (Fig. 24).

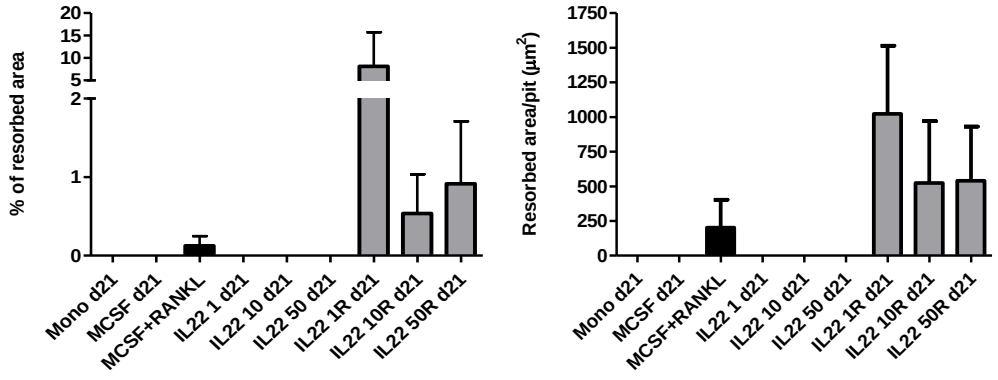

Fig. 24 – IL-22 optimization. Percentage of resorbed area and resorbed area per pit under unstimulated and stimulated conditions. Median values are shown with 75% percentile. Results were analyzed with Wilcoxon matched pairs test. *p* values lower than 0.05 are considered statistically significant. Mono – monocytes; M-CSF – macrophage colony-stimulating factor; RANKL – receptor activator of nuclear factor kappa-B ligand; IL – interleukin; IL22 1 – IL-22 at 1 ng/mL; IL22 10 – IL-22 at 10 ng/mL; IL22 50 – IL-22 at 50 ng/mL. IL22 1R – IL-22 at 1 ng/mL with RANKL; IL22 10R – IL-22 at 10 ng/mL with RANKL; IL22 50R – IL-22 at 50 ng/mL with RANKL; d21 – day 21.

After this optimization, the concentration selected was IL-22 at 10 ng/mL, because of the values obtained in MTT viability assays that were performed at days 7 and 21 of the experiment.

All the measurements done for IL-22 optimization were done for the celecoxib part of the assay too. In pre-OC number is possible to observe a higher value in the condition with celecoxib at 1 ng/mL with IL-22 and RANKL, there is no statistical significance however as seen in Fig. 25. OC number is also higher in that condition. The other conditions have similar values. The only conditions with OCs were the ones with the presence of RANKL. The nuclei number per OC is higher in celecoxib at 1 and 10 ng/mL with IL-22 and RANKL, when comparing with the positive control.

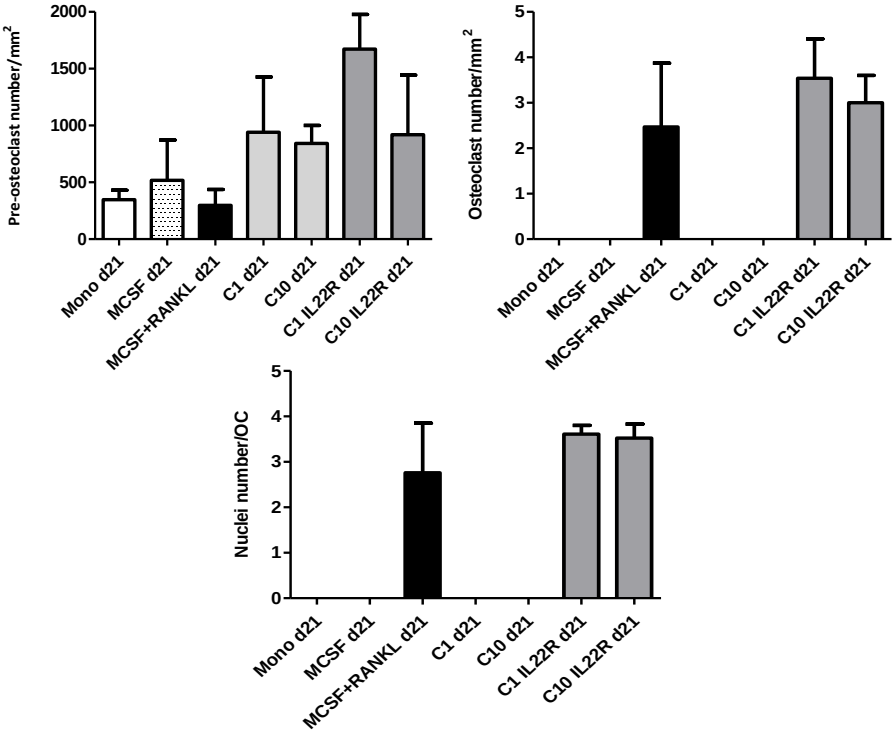

Fig. 25 – Celecoxib stimulation. Number of pre-OC, OC and nuclei per OC under unstimulated and stimulated conditions. Median values are shown with 75% percentile. Results were analyzed with Wilcoxon matched pairs test. *p* values lower than 0.05 are considered statistically significant. Mono – monocytes; M-CSF – macrophage colony-stimulating factor; RANKL – receptor activator of nuclear factor kappa-B ligand; C1 – celecoxib at 1 ng/mL; C10 – celecoxib at 10 ng/mL; IL22R – interleukin 22 at 10 ng/mL with RANKL; d21 – day 21.

In terms of number of pits and number of pits per OC the condition celecoxib at 1 ng/mL with IL-22 and RANKL still leads the values when comparing with the remaining ones as shown in Fig. 26. Positive control has more pits and as consequence more pits per OC than celecoxib at 10 ng/mL with IL-22 and RANKL.

When comparing the percentage of resorbed area and resorbed area per pit, it is possible to notice once again that celecoxib at 1 ng/mL with IL-22 and RANKL has the higher value. However this time celecoxib at 10 ng/mL with IL-22 and RANKL have considerable less area resorbed than the positive control (Fig. 27).

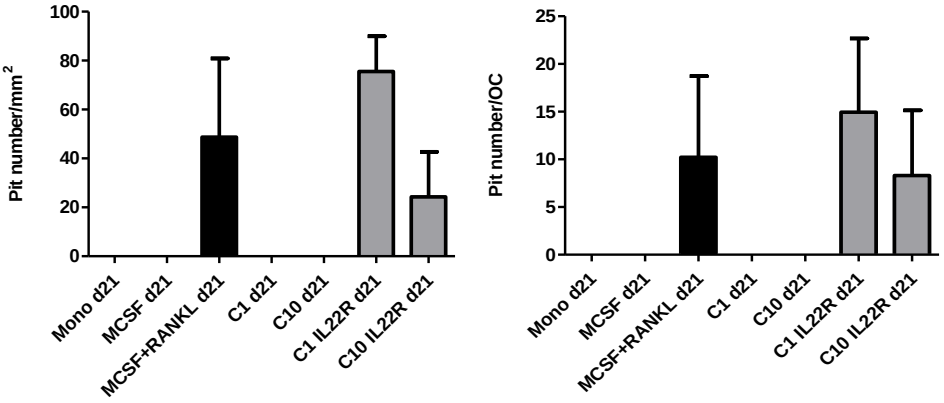

Fig. 26 – Celecoxib stimulation. Pit number and pit number per OC under unstimulated and stimulated conditions. Median values are shown with 75% percentile. Results were analyzed with Wilcoxon matched pairs test. *p* values lower than 0.05 are considered statistically significant. Mono – monocytes; M-CSF – macrophage colony-stimulating factor; RANKL – receptor activator of nuclear factor kappa-B ligand; C1 – celecoxib at 1 ng/mL; C10 – celecoxib at 10 ng/mL; IL22R – interleukin 22 at 10 ng/mL with RANKL; d21 – day 21.

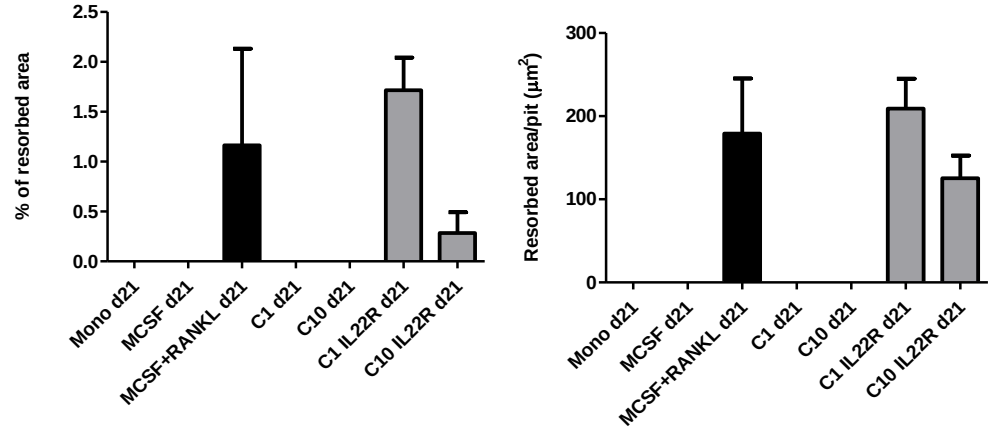

Fig. 27 – Celecoxib stimulation. Percentage of resorbed area and resorbed area per pit under unstimulated and stimulated conditions. Median values are shown with 75% percentile. Results were analyzed with Wilcoxon matched pairs test. *p* values lower than 0.05 are considered statistically significant. Mono – monocytes; M-CSF – macrophage colony-stimulating factor; RANKL – receptor activator of nuclear factor kappa-B ligand; C1 – celecoxib at 1 ng/mL; C10 – celecoxib at 10 ng/mL; IL22R – interleukin 22 at 10 ng/mL with RANKL; d21 – day 21

Gene expression

To characterize better the osteoclast assays, gene expression experiments were done. The genes analyzed were: CSF1R, CTSK, NFATc1, RANK and housekeeping gene 18S rRNA. However the RT-PCR results were not as expected. The first attempt was done using 15 ng/µL of cDNA with 0.25 µM of primer mix for each gene. The result can be observed in Fig. 28 for 18S gene as a representative gene. With the standards everything went well, but with the samples it is possible to notice amplification where the no template controls (NTCs) amplify too. For this reason the second attempt was using the double amount of primer mix testing the standards only, because maybe there was not enough primers to amplify the product properly. The results were better than the ones present in Fig. 28. In the third attempt with 0.5 µM of primer mix, all the samples were tested for 18S gene. The results were the same as Fig.28 and for that reason gene expression assays were suspended.

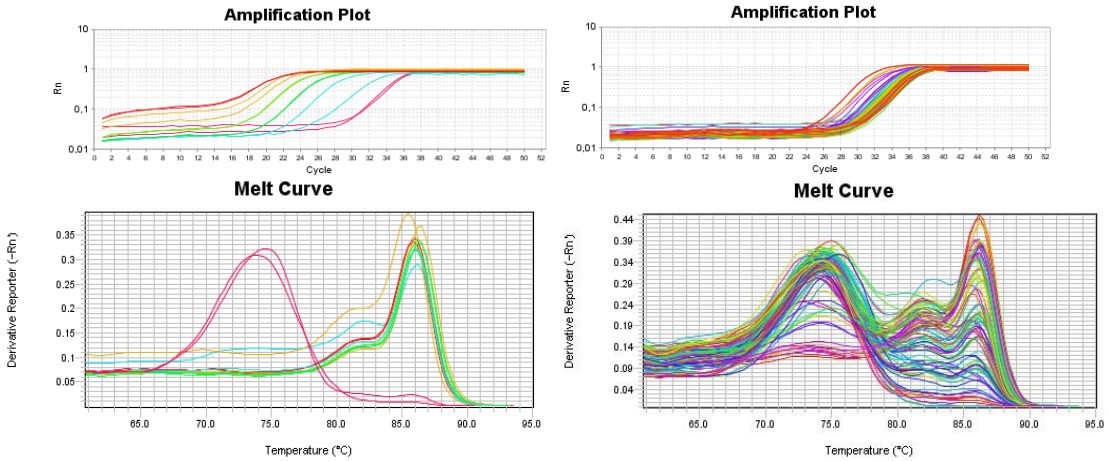

Fig. 28 – Amplification and melt curves for housekeeping gene 18S rRNA. Amplification plot at the left represents the curves of the standards and NTCs and on the right represents the curves for all the samples plus NTCs. The melt curve on the left represents standards and NTCs and on the right represents all the samples and NTCs. This RT-PCR was ran with 0.25 µM of primer mix.

III. Other results

Osteoblasts

In parallel with osteoclast assays, osteoblast assays were also done. Two different cell lines MG-63 and hFOB 1.19 were used with the characteristics displayed in Table III.1.

The first attempt to grow both cell lines was using Dulbecco's Modified Eagle Medium (DMEM), supplemented with 5000 U penicilin/streptomicin, 2 mM L-Glutamin, 50 µg/mL vitamin C, 50 mg/mL gentamicin, 15 mM HEPES and 10% FBS at 37°C for MG-63 and 33°C for hFOB 1.19, 5% CO_2. This medium seem to be accelerating the mineralization process and cells began to disappear at the same time perfect crystals appeared as shown in Fig. 29. The number of crystals increased day after day. The crystals were visible in MG-63 at day 2 and in hFOB 1.19 at day 5.

MG-63 cell line was recommended to be cultured with vitamin C, for that reason and to see if the crystal formation was vitamin C dependent, hFOB 1.19 cell line was cultured in a new DMEM medium without vitamin C. Both cell lines continued to exhibit crystal formation.

When the media were changed to what was recommended for each cell line: α-MEM supplemented with 5000 U penicilin/streptomicin, 2.5 µg/mL amphotericin B and 10% FBS for MG-63 and DMEM:F12 supplemented with 5000 U penicilin/streptomicin, 0.3 mg/mL G418 and 10% FBS for hFOB 1.19, crystals were not formed. In these two media cells grow normally as can be seen in Fig. 29.

MG-63 cells were cultured before in α-MEM supplemented with 5000 U penicilin/streptomicin, 2.5 µg/mL amphotericin B and 10% FBS with vitamin C. However cells did not adhere with efficiency. α-MEM medium was again added to the cells without vitamin C and their morphology and adhesion was normal (Fig.29).

Table III.1 – Characteristics of MG-63 and hFOB 1.19 cell lines.

Characteristics	MG-63	hFOB 1.19
Origin	Osteosarcoma	Fetus
Tissue	Bone	Bone
Growth mode	Adherent	Adherent
Morphology	Fibroblast	Fibroblast
Biosafey level	I	II
Growing temperature	37°C	33°C
Differentiation temperature	37°C	39°C
Passage number	5	2

MG-63 cell line was growing fast and healthy, so the next step was to take part of the cells to the mineralization medium: α-MEM supplemented with 5000 U penicilin/streptomicin, 2.5 µg/mL amphotericin B, 50 µg/mL vitamin C, 0.1 M β-glicerolphosphate, 2 mM L-Glutamin and 10% FBS. Under the stimulation of this new medium, mineralization was not observed. After one week of being in this medium, all cells remained the same as they were in the expansion medium previously.

The other cell line, hFOB 1.19 was having some problems in the expansion phase. In the several attempts made to grow these cells, they end up always contaminated. When adding amphotericin B to the medium, the contamination remained controlled, but always present. It was not possible to continue the study with these cells.

Having MG-63 incapable of mineralize and hFOB 1.19 contaminated, this study was suspended. The main goal was to differentiate the cells and stimulate them with IL-22 and celecoxib to investigate the osteoblast role, since the osteoclast part was already explored.

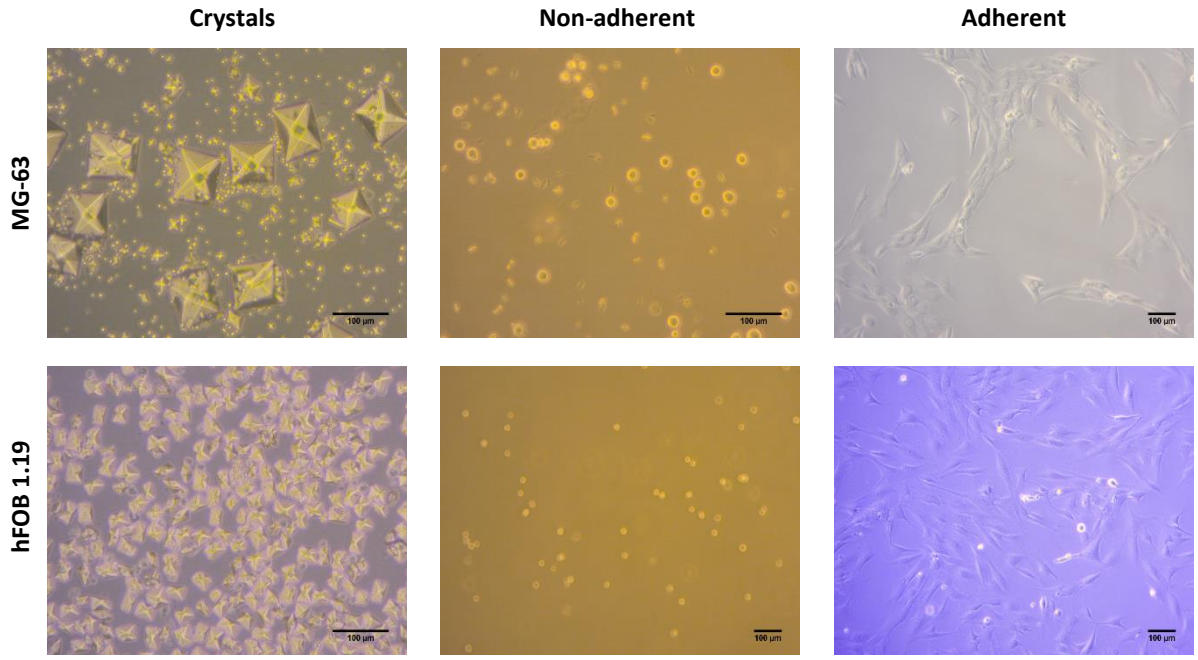

Fig. 29 – Osteoblast cells: MG-63 and hFOB 1.19 cell lines. Presence of crystals and non-adherent and adherent morphology. Scale bar corresponds to 100 µm.

Animal mouse model of spondyloarthritis

During this thesis a preliminary study using an animal model was also done. The animal mouse model is a model of spondyloarthritis. This strain present as phenotype hunchback, crinkled tail and deformed paws as the disease evolves as showed in Fig.30.

The model was new, so when animals became old (around 33 weeks old), they were euthanized and during the necropsy all the samples needed were collected, such as blood, paws, vertebrae, liver, spleen, small and large intestines. All the organs were processed for histology. Hematoxylin and eosin (H&E) staining was done in order to understand better the model and the inflammation pattern (Fig. 31).

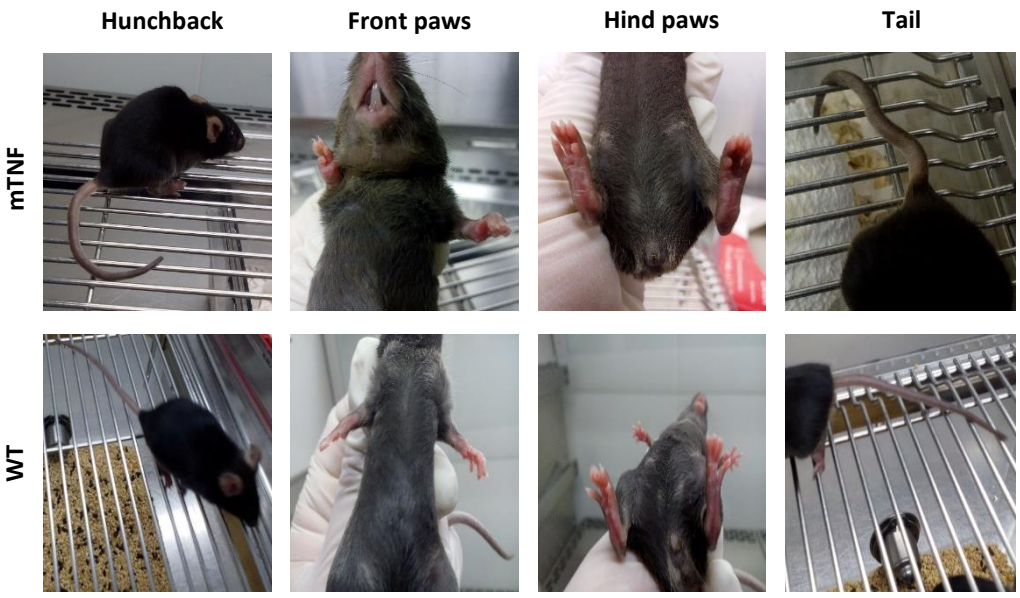

Fig. 30 – Phenotype differences between a membrane bound TNF and a wild-type mouse. Membrane bound TNF mouse presents hunchback, front and hind paws deformed and swollen and crinkled tail. Wild-type mouse does not present any of these features. Membrane bound TNF mouse in the photos has 21 weeks old. mTNF – membrane bound TNF; WT – wild-type.

In Fig. 31 is possible to notice inflammatory infiltrate (black arrows) in all images, except G, H and I. In image A inflammatory infiltrate is all over the footpad and cartilage erosion is present as well (black circle). When observing image B inflammatory infiltrate is located in the periarticular area. Image C displays inflammatory infiltrate closer to the growth plate and also cartilage erosion (black circle). In image D is also possible to visualize the skin thickening, which is not a characteristic in healthy animals. In images E and F, inflammatory infiltrate is present above and below the intervertebral disc, respectively. In image G no inflammatory infiltrate was found and is possible to distinguish between white and red pulp in the spleen. In image H the liver displays a normal morphology, with healthy hepatocytes and finally in image I, small intestine shows villi and micro villi with normal features.

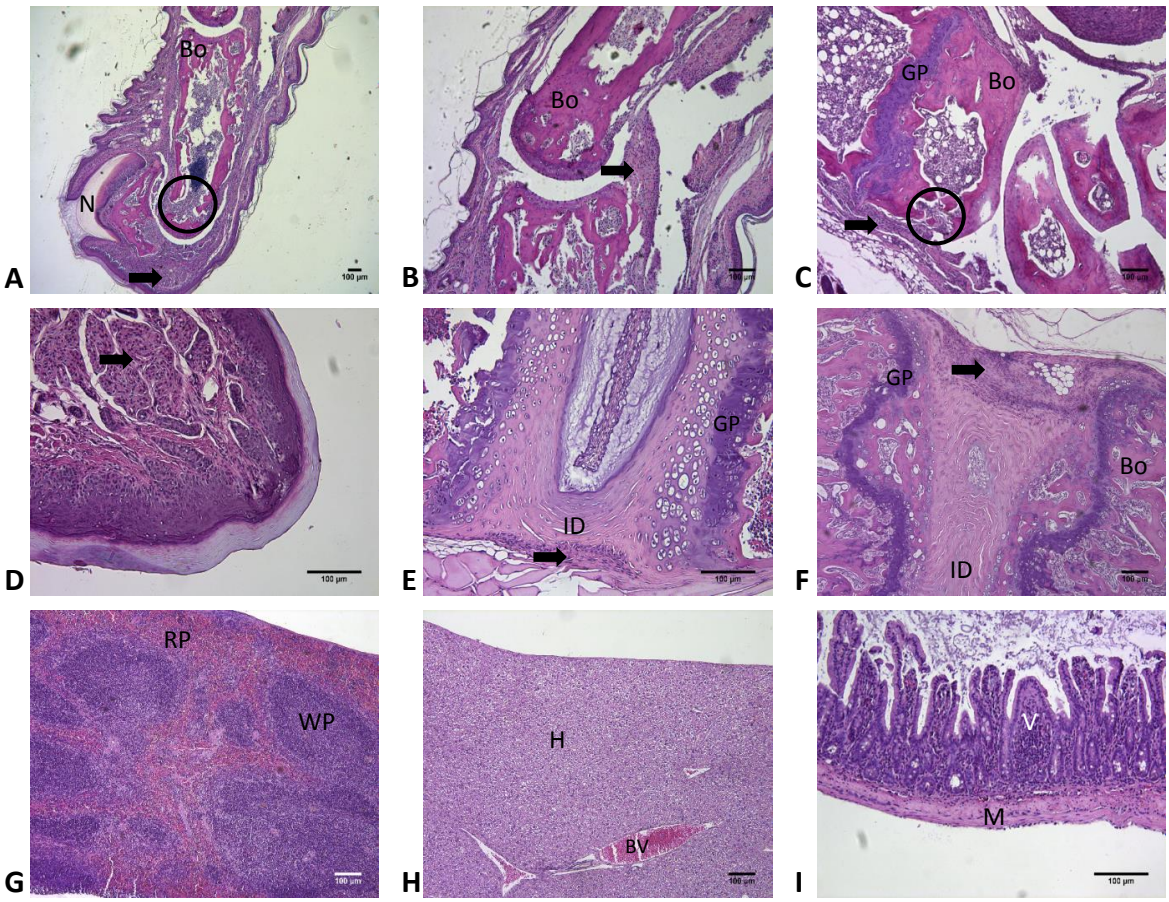

Fig. 31 – H&E staining. A – left front paw: digit with nail; B – left front paw: digit phalanx; C – left hind paw: calcaneus area; D – footpad; E – L3/L4 vertebrae transition; F – tail vertebrae; G – spleen; H – liver; I – small intestine. Black arrows represent inflammatory infiltrate; Black circles represent bone and cartilage erosion. Bo – Bone; N – nail; GP – growth plate; ID – intervertebral disc; RP – red pulp; WP – white pulp; H – hepatocytes; BV – blood vessel; V – villi; M – muscle; Each slide has 3 µm of thickness. Scale bar corresponds to 100 µm.

Immunohistochemistry (IHC), was also done for several antibodies. The selected antibodies were CD3 (T cell marker), CD19 (B cell marker), CD68 (monocyte/macrophage marker), CD163 (monocyte/macrophage marker) and SOST (osteocyte marker). An enzymatic antigen retrieval technique was used with Envision anti-rabbit as secondary antibody and hematoxylin counterstain. All the protocols are still under optimization. In Fig. 32 several images of IHC are displayed. All the stainings were performed using spleen, front and hind paws of the animal. In blue/purple is the background stained with hematoxylin and in brown/orange is present the antibody marking. In the spleen is possible to observe the T cell, B cell and macrophage marking in the red pulp. In both paws is detected a great inflammation

area. In left front paws is visible the inflammatory infiltrate in bone marrow. In left hind paws the inflammatory infiltrate is also visible in the footpads.

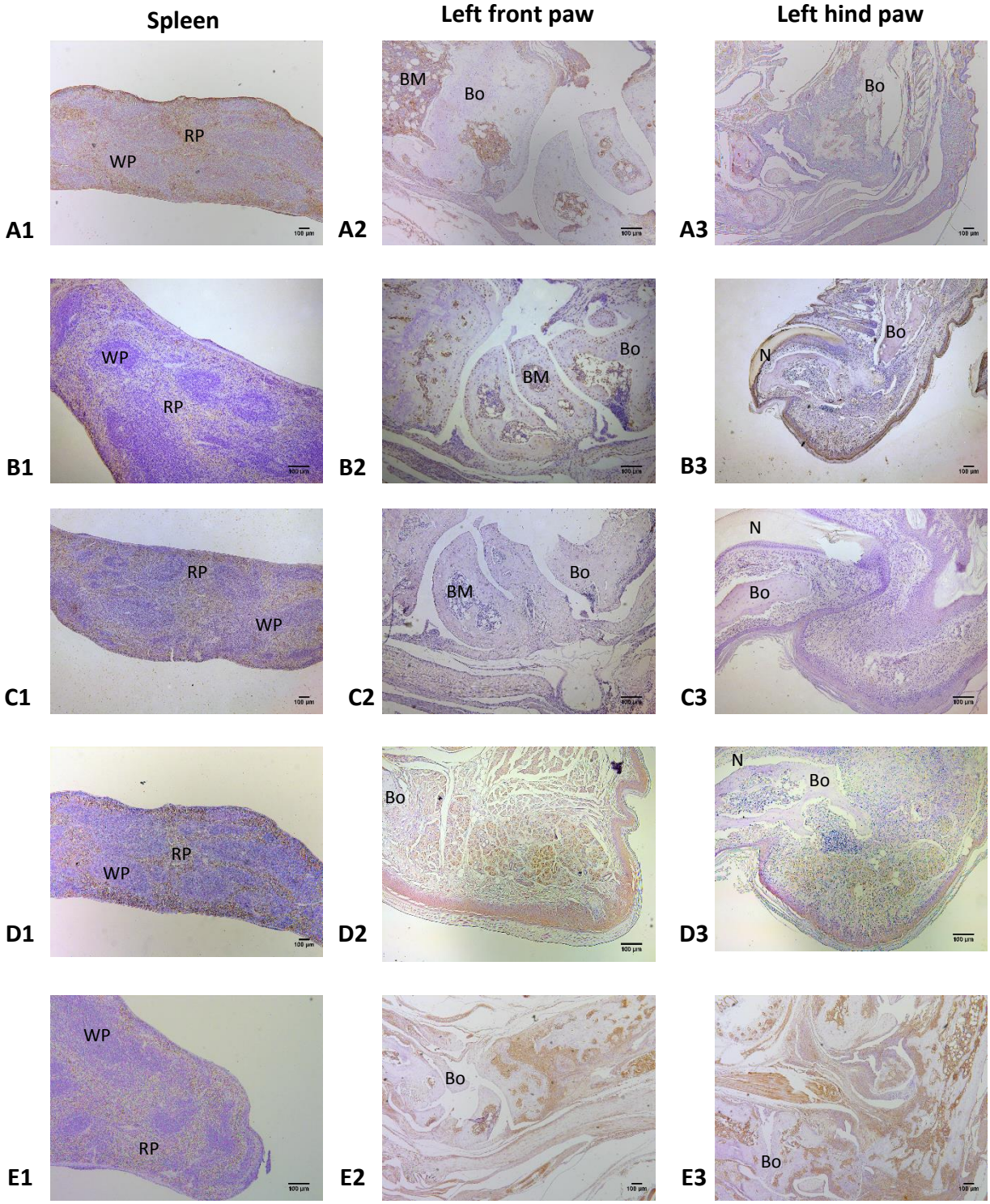

Fig. 32 – IHC staining in spleen and in left front and hind paws. A1-A3: CD3 marker; B1-B3: CD19 marker; C1-C3: CD68 marker; D1-D3: CD163 marker; E1-E3: SOST marker. Spleen was the control used in each IHC staining. RP – red pulp; WP – white pulp; BM – bone marrow; Bo – bone; N – nail; Each slide has 3 µm of thickness. Scale bar corresponds to 100 µm.

DISCUSSION

PsA is a seronegative spondyloarthritis characterized by bone formation and erosions. Enthesis are the most frequent affected areas showing increased bone formation, namely at the insertion of Achilles tendon. The common treatment for these patients is NSAID therapy and celecoxib is often used. Although PsA clinical trials using NSAIDs are scarce, in one study, celecoxib 400 mg and 200 mg significantly improved the symptoms of PsA in flare, after 2 weeks of treatment, when compared with placebo (Kivitz et al. 2007). Furthermore NSAIDs might have a potential inhibitory effect on new bone formation as highlighted in the study by Wanders et al (Wanders et al. 2005). IL-22 is a pro-inflammatory cytokine that plays a role in PsA and in bone metabolism. This cytokine seems to act in the pannus formation and as an osteoclastogenic factor (Wolk et al. 2006), (Ikeuchi et al. 2005), (Boniface et al. 2011), (Geboes et al. 2009). In this context is expected that patients under NSAID therapy will have less bone formation through prostaglandin inhibition and cytokine modulation.

The aim of this study is to understand differences in bone metabolism parameters, cytokines and prostaglandins in PsA and the effect of NSAIDs and IL-22 role in osteoclastogenesis.

Biomarkers and cytokines of bone metabolism

PsA patients who were not under NSAID therapy were recruited and for the paired study a second sample was collected for only 12 patients under NSAID therapy. Patients without NSAID therapy had a median age of 48.5 years, 2.5 years of symptoms duration and were predominantly men (Table I.1). Only 16% were positive for HLA-B27, which agrees with Ruiz et al study, where they mention that 72.7% of all the PsA patients analyzed were negative for the antigen (Ruiz, Azevedo, and Lupi 2012). The majority of patients had axial, peripheral and entheseal involvement, which is characteristic of PsA pathology. ESR and CRP markers were expected to be decreased in patients under NSAID therapy, however the *p* value is around 1, which indicates that values are similar before and after therapy (Tables I.1 and I.2). As healthy controls, 23

donors were recruited (12 for paired study), age and gender matched (Tables I.1 and I.2).

Biomarkers and cytokines of bone metabolism involved in PsA pathogenesis were measured in PsA, AS and healthy controls' serum. In this study the levels of CTX-I were elevated in controls when comparing with PsA patients and P1NP levels were increased in AS patients in comparison with controls. CTX-I/P1NP ratio showed decreased levels in both diseases (Fig. 11). This might indicate that this PsA population does not have significant bone resorption, because of the low CTX-I levels and show some bone formation but possible less than what is seen in AS. Grisar et al study demonstrated that CTX-I levels in PsA are higher than in controls (Grisar et al. 2002). Probably the patients recruited to our study had a stable disease. In Muntean et al study, AS patients also displayed higher levels of CTX-I when comparing with healthy controls (Muntean et al. 2011). Concerning P1NP levels, Acebes et al study reveal that in AS patients no statistical difference was found in comparison with controls (Acebes et al. 1999). The sample size in the present study is small (6 AS patients), so the results can differ and require confirmation in a larger population.

Serum levels of sRANKL and OPG were measured to evaluate bone resorption and formation as well. sRANKL is essential to osteoclastogenesis since it binds to RANK, which promotes osteoclast differentiation. OPG is an osteoclastogenesis inhibitor as it prevents RANKL and RANK binding (Florencio-silva et al. 2015), (Raggatt and Partridge 2010), (Cappariello et al. 2014). While sRANKL levels were similar between groups, OPG levels were increased in PsA patients (Fig. 12) suggesting that the decrease in bone resorption might be due to increased levels of OPG in PsA. In sRANKL/OPG ratio AS patients have an increase when comparing with PsA patients. Studies differ in this matter, on one hand Chandran et al, say that sRANKL and OPG levels are elevated in PsA patients when comparing with controls, on the other hand Dalbeth et al, show no differences between those levels and healthy controls (Chandran et al. 2010), (Dalbeth et al. 2010). When comparing AS patients and healthy controls some discrepancies are also found. Chen et al study shows elevated sRANKL and OPG levels in AS patients but Klingberg et al found lower sRANKL levels and lower sRANKL/OPG ratio in AS patients in comparison with controls (Chen et al. 2010),

(Klingberg et al. 2014). Taylan et al even found lower OPG levels but higher sRANKL/OPG ratio in AS patients (Taylan, Sari, Akinci, et al. 2012).

DKK-1 and SOST, Wnt signaling pathway inhibitors, play an important role in osteoblast differentiation, since this pathway is essential to osteoblast differentiation and function (Florencio-silva et al. 2015), (Raggatt and Partridge 2010), (Pinzone et al. 2014). These two markers were assessed in this study. No significant differences in DKK-1 levels were found between groups, although patients seem to have higher levels of the protein (Fig. 13). In Dalbeth et al study, DKK-1 levels were significantly increased in PsA patients in comparison with controls (Dalbeth et al. 2010). In the present study the bone resorption pathways might not be much active in patients. When comparing AS results with published studies, Daoussis et al show elevated DKK-1 levels in AS patients under anti-TNF therapy when comparing with controls and also increased levels in AS patients under anti-TNF therapy in comparison with PsA patients (Daoussis et al. 2010). However Kwon et al found decreased levels in AS patients when comparing with healthy controls (Kwon et al. 2012). Ustun et al also found decreased levels in AS patients, but were not statistically significant (Ustun et al. 2014). Taylan et al saw that AS patients and healthy controls did not show significant differences which agrees with this study (Taylan, Sari, Akinci, et al. 2012).

Regarding SOST serum levels, it was found a significant decrease in both patients' groups when comparing with controls (Fig. 13). This difference show once more that resorption is not very active in disease and osteoblastogenesis is less suppressed. These results are profoundly relevant, as until now no published work found this relation in PsA patients. In AS patients, studies show a decrease in SOST levels when comparing with controls. Appel et al found decreased levels in AS patients without anti-TNF therapy and Ustun et al show also a decrease in those levels, both works are in agreement with this study (Appel et al. 2009), (Ustun et al. 2014).

Pro-inflammatory cytokines IL-22 and IL-23 are relevant in the inflammation axis in PsA disease (Mitra, Raychaudhuri, and Raychaudhuri 2012), (El Hadidi et al. 2008). No significant differences were found in IL-22 and IL-23 levels between patients and controls, although IL-22 levels seem to be decreased in patients (Fig. 14). In published works both IL-22 and IL-23 cytokine levels are increased in patients when comparing with controls. For IL-22, Benham et al and Zhang et al show increased levels

in PsA and AS patients, respectively, in comparison with controls (Benham et al. 2013), (Zhang et al. 2012). As for IL-23, El Hadidi et al found increased serum levels in PsA patients, Taylan et al show higher levels in AS patients and Przepiera-Bedzak et al observed increased levels in both PsA and AS patients, always comparing with healthy controls (El Hadidi et al. 2008), (Taylan, Sari, Kozaci, et al. 2012), (Przepiera-Będzak, Fischer, and Brzosko 2015). Probably using a higher number of samples could evidence differences between healthy controls and patients in this study.

PGE_2 is an important prostaglandin in PsA disease when considering NSAID therapy through COX-2 inhibition. This prostaglandin has pro-inflammatory activity and by using NSAIDs such as celecoxib, COX-2 is specifically inhibited, resulting in prostaglandin decrease (Kalinski 2012), (Tive 2000). When looking to Fig. 14, it is possible to notice that patients have lower levels of PGE_2 than controls. It is important to refer that all samples, 9% of which were receiving NSAIDs, were collected without indomethacin. Indomethacin seems to stop PGE_2 activity, preserving the original levels of this prostaglandin in the blood when collected (Rhind et al. 1999). Concerning PsA disease, no published works refer to PGE_2 serum quantifications and in AS patients only Ji et al work was found, where they observe significant differences between AS patients before and after taking tripterygium glycosides tablets. In that study PGE_2 levels decrease significantly when comparing with controls (Ji et al. 2015). In RA disease it is known that PGE_2 has pathological effect and for that reason has been a potential therapy target. In RA, PGE_2 levels seem to be higher than in controls (Gheorghe et al. 2012).

When PsA patients were paired, before and after NSAID therapy, no statistical significance was found. CTX-I and P1NP levels are very similar before and after therapy as shown in Fig. 15. When analyzing its ratio, before and after therapy display constant values.

sRANKL, OPG and sRANKL/OPG ratio levels are constant before and after NSAID therapy with a slightly increase in sRANKL/OPG ratio after therapy (Fig. 16).

Regarding Wnt pathway inhibitors, DKK-1 and SOST levels are not statistically significant. DKK-1 levels show no differences between before, after and controls and SOST levels seem to be increased in healthy controls only as shown in Fig. 17. DKK-1 levels in Dalbeth et al study are elevated in PsA patients (Dalbeth et al. 2010).

Pro-inflammatory cytokines, IL-22 an IL-23 have similar quantifications before and after therapy and the controls have a disperse pattern (Fig. 18). Concerning PGE_2 levels, they seem to be the same or slightly higher after therapy, which may not be logical. Patients under PGE_2 therapy should have COX-2 pathway blocked and consequently lower levels of circling PGE_2 in blood. Like before these samples were collected without indomethacin, which may explain these results.

Osteoclast assays

The effect of different IL-22 concentrations in the number of pre-OC, OC and nuclei per OC after TRAP staining was assessed. IL-22 concentrations, in the absence of RANKL, are able to increase the number of pre-OC (Fig. 22). Similarly to M-CSF, IL-22 10 ng/mL was associated with an increase in OC number. Nuclei number per OC is generally the same throughout all conditions. While OCs are usually absent in unstimulated conditions and when present the number is lower when comparing with other conditions, these results indicate spontaneous differentiation of monocytes into pre-osteoclast and then into osteoclasts. No statistically significance ($p<0.05$) was found between the studied conditions. No published study mentions OCs developing in unstimulated conditions. A possible explanation is through integrins. Pre-OCs when attaching to bone slices through integrins may activate pathways that can induce osteoclast differentiation. In Stupack and Cheresh study, they say integrins can transmit pro-survival signals when interacting with matrix-residing ligand, which can be the cause for OCs differentiation in unstimulated conditions (Stupack and Cheresh 2002).

After resorption pit assay with toluidine blue, pit number, pit number per OC, percentage of resorbed area and resorbed area per pit were counted and measured. Pits were only observed in positive control M-CSF + RANKL and in IL-22 stimulation with RANKL, concluding that in this experiment, for osteoclastogenesis and consequently bone resorption to take place RANKL is a crucial factor. The number of pits is higher at IL-22 1 ng/mL concentration with RANKL and the other values are similar to positive control as seen in Fig. 23. The Pit number per OC is also higher at IL-22 1 ng/mL concentration with RANKL. After analyzing these two previous results is expected that IL-22 1 ng/mL with RANKL has the highest percentage of resorbed area and resorbed area per pit, which was in fact confirmed. These results show no significance in

statistical matters ($p<0.05$). IL-22 seems to have an osteoclastogenic role potentiating RANKL effect. In Kim et al study, they found that IL-22 preexposed RA synovial fibroblasts, directly induced osteoclastogenesis by monocytes in the absence of RANKL. They also showed IL-22 osteoclastogenic role when coculturing purified PBMCs with IL-22 preexposed RA synovial fibroblasts and M-CSF in the absence of RANKL (K. W. Kim et al. 2012). Other work done by Kim et al demonstrated IL-22 osteoclastogenic potential using fibroblast-like synoviocytes in RA (K.-W. Kim et al. 2015). After this dose finding experiments, IL-22 at 10 ng/mL was selected based in the results obtained in MTT viability assays.

TRAP staining and resorption pit assays were equally done for this next experiment. Because celecoxib is a commonly used NSAID in PsA disease, it was interesting to understand if in cell cultures this drug had any influence in osteoclasts. Conditions with two different concentrations of celecoxib alone and celecoxib with IL-22 (10 ng/mL) and RANKL (100 ng/mL) were studied.

In pre-OC number, higher values are observed in celecoxib stimulation, particularly in celecoxib 1 ng/mL with IL-22 and RANKL as can be seen in Fig. 25. OC number is also higher in that condition and in nuclei number per OC all conditions have similar values. OC number and nuclei number per OC, were significantly increased in these conditions when comparing with the remaining were no effect was observed.

When comparing results in resorption pit assays, celecoxib at 1 ng/mL with IL-22 and RANKL lead the values, in comparison with the remaining ones (Fig. 26). The percentage of resorbed area and resorbed area per pit has highest values in the celecoxib 1 ng/mL with IL-22 and RANKL condition. There is a great decrease in celecoxib 10 ng/mL with IL-22 and RANKL condition when comparing with positive control. As observed before in IL-22 optimization, the only conditions with pits and resorption were the ones with RANKL stimulation. In this case even OCs were only present in RANKL conditions. The number of pits, number of pits per OC and resorbed area are higher in the lower celecoxib concentration. When increasing this concentration 10 times, all this values decrease, which is predicted by Igarashi et al, since celecoxib acts as bone resorption inhibitor (Igarashi, Woo, and Stern 2002).

When comparing IL-22 with celecoxib results concerning OC number is evident the decrease from IL-22 to celecoxib with IL-22 values, which indicates that celecoxib

managed to stop IL-22 osteoclastic action. Although pit number and pit number per OC are higher in celecoxib stimulation than in IL-22, when comparing resorption levels, celecoxib registers a decrease in bone resorption. In Igarashi et al work, celecoxib is presented as an important bone resorption inhibitor, through COX-2 inhibition and consequently prostaglandins (Igarashi, Woo, and Stern 2002). However other study reports that NSAIDs like ketorolac can alter bone remodeling by reducing cell maturation, its longevity and biochemical machinery that is necessary to mineralize the deposited extracellular matrix (De Luna-Bertos et al. 2013). This previous study enhances the NSAID capacity of inhibit bone formation.

RNA from all conditions was extracted for cDNA synthesis and gene expression by RT-PCR means. To characterize better the effect of these conditions on osteoclastogenesis the following genes were selected for gene expression analysis: CSF1R, CTSK, NFATc1, RANK and housekeeping gene 18S rRNA. The RT-PCR results did not occurred as expected. In the first runs 15 ng/µL of cDNA with 0.25 µM of primer mix for each gene was used. This resulted in non-specific amplification with the samples amplifying in NTC area as shown in Fig. 28. The second attempt was made using 0.50 µM of primer mix, thinking that maybe there was not enough primers to amplify the product. In this attempt the results were better, but only standards were tested. In order to investigate if in samples the problem was resolved the third attempt was made with the same conditions but in samples also. Unfortunately the results were similar to Fig. 28 and gene expression study was suspended.

To understand the reason behind this problem, RNA was again quantified by nanodrop. As before the majority of samples showed a good concentration but bad 260:280 and 260:230 ratios. 260:280 ratio measures the possible contamination with nucleic acids and should be around 2.0 for RNA. 260:230 ratio measures the possible contamination with phenolic solutions and should be around 2.0-2.3 (Thermo Fisher Scientific 2011). RNA extraction was performed using NZYol reagent, which is a phenolic solution. That may be the reason why samples were not obtaining good 260:230 ratios. To further investigate these results, a clean-up with Zymo kit in columns was done for 5 samples (protocol available in ANNEX V). After this clean up, all samples were quantified again in nanodrop. In all samples RNA concentration was

decreased by 100 times and ratios were still the same. Still wondering what was happening, an electrophoresis gel agarose was performed. In theory 2 bands should be visible in RNA runs, but the only bands visible in the gel were in the ladder lanes. This means that the RNA extracted have its integrity compromised. Something happened during RNA extraction that could not permit an efficient cDNA synthesis that resulted in poor RT-PCR curves.

Osteoblast cultures

Aiming to understand the effect of IL-22 and celecoxib on osteoblastogenesis, osteoblast cell lines were selected to culture in different conditions. MG-63 and hFOB 1.19 cell lines (Table III.1) were cultured first in DMEM, supplemented with 5000 U penicilin/streptomicin, 2 mM L-Glutamin, 50 µg/mL vitamin C, 50 mg/mL gentamicin, 15 mM HEPES and 10% FBS at 37°C for MG-63 and 33°C for hFOB 1.19, 5% CO_2. This medium seem to accelerate mineralization process and cells began to synthetize crystals as seen in Fig. 29. As the number of crystals increased, the number of cells decreased. Because of temperature differences, crystals appeared in MG-63 medium at day 2 and at day 5 in hFOB 1.19 medium. Crystal morphology indicates that maybe calcium oxalate crystals are present in the medium when comparing with other calcium oxalate images (Sun et al. 2015). The current hypothesis is therefore that calcium oxalate crystals were formed in these media. It is known for long time that hydroxyapatite is the crystal present in bone formation process (Lian and Stein 1995). However this is not the crystal observed in the culture media. Calcium oxalate is present in kidney stones (Finkielstein and Goldfarb 2006). The hypothesis is that somehow the medium components together with cell metabolism created these crystals. When the medium was cultured alone, no crystals were visible, this means cell metabolism is necessary for them to appear. Vitamin C precipitation was also a hypothesis, but when culturing cells without and with vitamin C in the first medium, both conditions exhibited crystals. This means that crystal formation is not vitamin C dependent.

Culture medium was changed to what was recommended by companies for each cell line and crystals were not observed, cells grow perfectly normal as shown in Fig.29.

MG-63 cell line was the first to get a steady growth, so the next step was to differentiate the cells. Mineralization was not observed and all cells remained the same as they were in the previous medium. Mineralization in this cell line was observed by other groups studying NSAIDs effects in osteoblasts, allografts, natural compounds testing and biomaterials (De Luna-Bertos et al. 2013), (Lafzi et al. 2015), (Lin et al. 2014), (Fan, Yang, and Bi 2015). For unknown reasons, some groups can promote MG-63 mineralization. Further work needs to be done to solve this.

With hFOB.19 cell line, some problems due to contamination were observed. At the second passage cells always presented some contamination. When adding 2.5µg/mL of amphotericin B, the contamination becomes controlled, but always present. Cells were even treated with 5.0 µg/mL of amphotericin diluted in PBS before each passage in order to reduce the contamination. It was not possible to continue the study with these cells. This cell line, like MG-63 is extremely used for biomaterials and compound testing (Karolina et al. 2015), (Osteoblast and Line 2015), (Przekora and Ginalska 2015). When culturing these cells, G418 is recommended to add in the medium, this substance is a disulfate salt that is recommended to use when maintaining eukaryotic cells that were transfected with neomycin resistance genes. This antibiotic has similar structure to gentamicin, neomycin and kanamycin (Finley 2012). ATCC, a company that provides this cell line says that these cells were selected in the presence of 0.6 mg/mL G418 and were established by transfection of limb tissue obtained from a miscarriage with temperature sensitive and neomycin resistance vectors. This may be the main reason why these cells are so susceptible to contamination (ATCC 2015).

Since MG-63 cells were incapable of mineralize and hFOB 1.19 cells were contaminated, this study was suspended.

Animal mouse model of spondyloarthritis

A preliminary study using an animal model was also done. The animal model mouse is a model of spondyloarthritis which presents hunchback, crinkled tail and deformed paws phenotype (Fig.30).

Old animals of this strain were euthanized and organ samples were collected to analyze. H&E and IHC stainings were done to several samples. H&E staining included paws, L3/L4 vertebrae and tail vertebrae, spleen, liver and small intestine. IHC staining included only paws and spleen.

In H&E staining is possible to notice inflammatory infiltrate in every slide, except spleen, liver and small intestine that showed no histological changes (Fig. 31). Bone and cartilage erosions were present in left front and hind paws as well. When comparing this mouse model with other models, it is possible to notice some advantages. For instances, this strain does not develop inflammatory bowel disease (IBD) like TNFdeltaARE strain. This characteristic enables to maintain the animal in experiments during longer periods, since the disease development characteristics are less severe (Alexopoulou, Pasparakis, and Kollias 1997), (Kontoyiannis et al. 1999). Some strains to develop the correct genotype and phenotype accordingly to the disease in study need to be induced, this is the case of collagen induced arthritis (CIA) mice (Brand, Latham, and Rosloniec 2007). In mTNF mice, all animals have total disease penetrance, manifesting the same symptom severity (van Duivenvoorde, Leonie M., van Tok, Melissa N., Baeten 2013).

In IHC staining, five markers were used: CD3 (T cell marker), CD19 (B cell marker), CD68 (monocyte/macrophage marker), CD163 (monocyte/macrophage marker) and SOST (osteocyte marker). In brown/orange is present the antibody marking and in blue/purple is the background with hematoxylin counterstain (Fig. 32). All protocols are still under optimization. In CD3 marking is possible to find T cells in spleen's red pulp and in both left paws in bone marrow (A1-A3 in Fig.32) (Shami et al. 2015). CD19 marking B cells was observed in spleen's red pulp and in both left paws bone marrow as well (B1-B3 in Fig.32). In Fig. 32 B3, is visible some marking closer to the nail and at the footpad (Guo et al. 2015). CD68 and CD163 antibodies mark the same type of cells, macrophages (Cojocaru et al. 2012), (Lau, Chu, and Weiss 2004). CD163 seem to have better results in staining macrophages, that is the reason why,

sometimes both antibodies are used (Klein et al. 2014). The stainings mark spleen's red pulp and inflammatory infiltrate in footpads (C1-C3 and D1-D3 in Fig. 32). Finally SOST is a marker of osteocytes and stained spleen's red pulp lightly and inflammatory infiltrate in both paws (E1-E3 in Fig. 32) (van Bezooijen et al. 2004). Having spleen positive staining for SOST is not normal, but because this staining is still under optimization and the marking is light, after optimizing the protocol, SOST marking for red pulp should disappear.

In conclusion, CTX-I and OPG quantifications suggest low bone resorption in PsA patients. SOST low levels in PsA patients resemble the AS patients ones previously reported. As a Wnt pathway inhibitor, SOST leads to decreased bone formation. In PsA patients low levels of SOST means less Wnt pathway inhibition, which might result in more bone formation. Osteoclast assays confirmed that RANKL is essential to osteoclastogenesis. This effect was potentiated by adding IL-22 in a concentration of 10ng/mL, in contrast celecoxib seems to have an inhibitor role at the same dose.

FUTURE WORK

The work developed in this thesis will be continued. Many aspects related to the future experimental set up were defined and preliminary requirements were guaranteed. One of this studies is the efficient differentiation of hFOB 1.19 cell line.

For differentiation, cells must be cultured DMEM:F12 (1:1) (Gibco, USA) supplemented with 5000 U penicilin/streptomicin (Invitrogen, UK), 50 µg/mL vitamin C (Fluka analytical, USA), 4 mM β-glicerolphosphate (Fluka analytical, USA), 2 mM L-Glutamin (Invitrogen, UK) and 10% FBS (Invitrogen, UK) at 39°C, 5% CO_2. Medium needs to be changed every three days.

The experimental design is divided in two parts: proliferation and differentiation phases. In the proliferation phase, cells grow to an optimum state during 1 week in order to go to the differentiation step. After reaching confluence and the cell density required for the experiment, cells are incubated in differentiation media for 14 days, in 24 well flat bottom plates (Corning Costar, USA) in unstimulated and stimulated conditions (Fig. 33). The unstimulated condition refers to addition of differentiation media only. The stimulated conditions are divided in six: **A)** Celecoxib 1 and 10 µM (Sigma-Aldrich, USA), **B)** TNF (1 ng/mL, R&D, USA) + IL-17A (10 and 50 ng/mL, eBioscience, USA), **C)** TNF + IL-22 (10 and 50 ng/mL, Peprotech, USA), **D)** IL-17A + IL-22, **E)** TNF + IL-17A + Celecoxib, **F)** TNF + IL-22 + Celecoxib and **G)** IL-17A + IL-22 + Celecoxib.

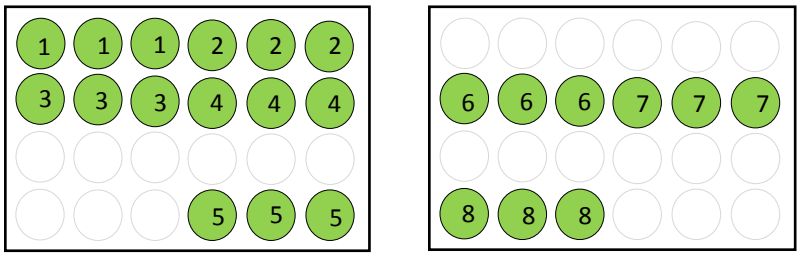

Fig. 33 – Design of 24 well culture plates with unstimulated and stimulated conditions. **Unstimulated condition**: 1) Differentiation media only; **Stimulated conditions**: 2) Celecoxib, 3) TNF+IL-17A, 4) TNF+IL-22, 5) IL-17A+IL-22, 6) TNF+IL-17A+Celecoxib, 7) TNF+IL-22+Celecoxib, 8) IL-17A+IL-22+Celecoxib.

After the differentiation period, cells are fixated with 10% paraformaldehyde (PFA, VWR, USA) in 0.1 M cacodylate buffer (Fluka analytical, USA) and some tests are performed such as MTT assays, alkaline phosphatase (ALP) activity and von Kossa staining. RNA from all conditions must be extracted for gene expression quantification.

Alkaline phosphatase activity

Alkaline phosphatase is a hydrolase enzyme that provides high amounts of phosphate needed for mineral deposition in the process of osteogenesis. Measuring its activity allows to know better the cell lines development and if there is any osteoformation.

To test this, 4% PFA (VWR, USA) is added to the wells with PBS 1x. Then a Fast Violet B Salt capsule (Sigma-Aldrich, USA) is dissolved in distilled water (solution A). Solution B is prepared by adding Naphtol AS-MX Phospate Alkaline Solution (Sigma-Aldrich, USA) to the solution A. PBS and PFA are removed from the wells and cells are incubated with solution B for 1h at RT in the dark. Cells are then washed with distilled water for 2 minutes at RT.

Von Kossa staining

For this staining the cells are incubated with 5% $AgNO_3$ (Sigma-Aldrich, USA) in water under UV light without cover for 1h at RT. Cells are washed with distilled water and then incubated with 5% sodium thiosulfate (Fluka analytical, USA) during 2 minutes and washed again. This test enables to verify the presence of calcium in each well.

After this procedures, RNA from all conditions should be collected and extracted, cDNA synthetized as previously done with osteoclasts and finally gene expression quantified by RT-PCR. The genes selected to this cell line are RUNX2, OSX, OCN, COL1A and 18S rRNA as housekeeping gene.

Other aspect that remains to optimize is the RT-PCR curves in osteoclast gene expression.

Inflammatory cytokines and biomarkers of bone metabolism

In the future, IL-6 is an interesting cytokine to quantify in the PsA patients' serum. IL-6 is a pro-inflammatory cytokine that was already studied in systemic lupus erythematosus and RA. In both diseases IL-6 production is increased and plays a crucial role (Tackey, Lipsky, and Illei 2004), (Srirangan and Choy 2010). In psoriasis IL-6 has been studied as well and along with its blockade (Atzeni et al. 2012). It would be important to quantify this protein in the PsA patients studied in this thesis to clarify and characterize better this disease.

REFERENCES

Acebes, C, C de la Piedra, M L Traba, M J Seibel, C García Martín, J Armas, and G Herrero-Beaumont. 1999. "Biochemical Markers of Bone Remodeling and Bone Sialoprotein in Ankylosing Spondylitis." *Clinica Chimica Acta; International Journal of Clinical Chemistry* 289 (1-2): 99–110.

Alexopoulou, Lena, Manolis Pasparakis, and George Kollias. 1997. "A Murine Transmembrane Tumor Necrosis Factor (TNF) Transgene Induces Arthritis by Cooperative p55/p75 TNF Receptor Signaling." *European Journal of Immunology* 27 (10): 2588–92.

Alvarez-Nemegyei, J., and J. J Canoso. 2006. "Heel Pain: Diagnosis and Treatment, Step by Step." *Cleveland Clinic Journal of Medicine* 73 (5): 465–71.

Amherd-Hoekstra, a., Helmut Näher, Hanns Martin Lorenz, and Alexander H. Enk. 2010. "Psoriasisarthritis: Ein Übersichtsartikel." *JDDG - Journal of the German Society of Dermatology* 8 (5): 332–40.

Appel, Heiner, Gisela Ruiz-Heiland, Joachim Listing, Jochen Zwerina, Martin Herrmann, Ruediger Mueller, Hildrun Haibel, et al. 2009. "Altered Skeletal Expression of Sclerostin and Its Link to Radiographic Progression in Ankylosing Spondylitis." *Arthritis and Rheumatism* 60 (11): 3257–62.

ATCC. 2015. "hFOB 1.19." Accessed July 19 2015. http://www.lgcstandards-atcc.org/products/all/CRL-11372.aspx?geo_country=pt#characteristics.

Atzeni, Fabiola, Donatella Ventura, Alberto Batticciotto, Laura Boccassini, and Piercarlo Sarzi-Puttini. 2012. "Interleukin 6 Blockade: Tocilizumab in Psoriatic Arthritis." *Journal of Rheumatology* 39 (SUPPL. 89): 97–99.

Barton, Anne C. 2002. "Genetic Epidemiology. Psoriatic Arthritis." *Arthritis Research* 4 (4): 247–51.

Bas, S, S Genevay, O Meyer, and C Gabay. 2003. “Anti-Cyclic Citrullinated Peptide Antibodies, IgM and IgA Rheumatoid Factors in the Diagnosis and Prognosis of Rheumatoid Arthritis.” *Rheumatology (Oxford, England)* 42 (5): 677–80.

Benham, Helen, Paul Norris, Jane Goodall, Mihir D Wechalekar, Oliver FitzGerald, Agnes Szentpetery, Malcolm Smith, Ranjeny Thomas, and Hill Gaston. 2013. “Th17 and Th22 Cells in Psoriatic Arthritis and Psoriasis.” *Arthritis Research & Therapy* 15 (5). Arthritis Research & Therapy: R136.

Boniface, Katia, François-xavier Bernard, Martine Garcia, Austin L Gurney, Jean-claude Lecron, Franck Morel, and Human Keratinocytes. 2011. “Proinflammatory Gene Expression and Migration of.” *The Journal of Immunology* 174: 3695–3702.

Brand, David D, Kary a Latham, and Edward F Rosloniec. 2007. “Collagen-Induced Arthritis.” *Nature Protocols* 2 (5): 1269–75.

Cappariello, Alfredo, Antonio Maurizi, Vimal Veeriah, and Anna Teti. 2014. “The Great Beauty of the Osteoclast.” *Archives of Biochemistry and Biophysics* 558. Elsevier Inc.: 70–78.

Chandran, Vinod, Richard J. Cook, Jonathan Edwin, Hua Shen, Fawnda J. Pellett, Sutharshini Shanmugarajah, Cheryl F. Rosen, and Dafna D. Gladman. 2010. “Soluble Biomarkers Differentiate Patients with Psoriatic Arthritis from Those with Psoriasis without Arthritis.” *Rheumatology* 49 (7): 1399–1405.

Chandran, Vinod, and Siba P. Raychaudhuri. 2010. “Geoepidemiology and Environmental Factors of Psoriasis and Psoriatic Arthritis.” *Journal of Autoimmunity* 34 (3). Elsevier Ltd: J314–21.

Chen, Chun Hsiung, Hung An Chen, Hsien Tzung Liao, Chin Hsiu Liu, Chang Youh Tsai, and Chung Tei Chou. 2010. “Soluble Receptor Activator of Nuclear Factor-kB Ligand (RANKL) and Osteoprotegerin in Ankylosing Spondylitis: OPG Is Associated with Poor Physical Mobility and Reflects Systemic Inflammation.” *Clinical Rheumatology* 29 (10): 1155–61.

Coiffier, Guillaume, Béatrice Bouvard, Florance Chopin, Emmanuel Biver, Thomas Funck-Brentano, Patrick Garnero, and Pascal Guggenbuhl. 2013. "Common Bone Turnover Markers in Rheumatoid Arthritis and Ankylosing Spondylitis: A Literature Review." *Joint, Bone, Spine : Revue Du Rhumatisme* 80 (3). Elsevier Masson SAS: 250–57.

Cojocaru, Elena, Mioara Trandafirescu, Magda Leon, C. Cotuţiu, and Liliana Foia. 2012. "Immunohistochemical Expression of Anti-CD68 Antibody in Atherosclerotic Plaque." *Romanian Journal of Morphology and Embryology* 53 (1): 61–66.

Dalbeth, Nicola, Bregina Pool, Timothy Smith, Karen E Callon, Maria Lobo, William J Taylor, Peter B Jones, Jillian Cornish, and Fiona M McQueen. 2010. "Circulating Mediators of Bone Remodeling in Psoriatic Arthritis: Implications for Disordered Osteoclastogenesis and Bone Erosion." *Arthritis Research & Therapy* 12 (4): R164.

Daoussis, Dimitrios, S. N C Liossis, Elena E. Solomou, Anastasia Tsanaktsi, Konstadina Bounia, Maria Karampetsou, Georgios Yiannopoulos, and Andrew P. Andonopoulos. 2010. "Evidence That Dkk-1 Is Dysfunctional in Ankylosing Spondylitis." *Arthritis and Rheumatism* 62 (1): 150–58.

De Luna-Bertos, E., J. Ramos-Torrecillas, O. Garcia-Martinez, a. Guildford, M. Santin, and C. Ruiz. 2013. "Therapeutic Doses of Nonsteroidal Anti-Inflammatory Drugs Inhibit Osteosarcoma MG-63 Osteoblast-like Cells Maturation, Viability, and Biomineralization Potential." *The Scientific World Journal* 2013 (2008).

Delmas, P. D., R. Eastell, P. Garnero, M. J. Seibel, and J. Stepan. 2000. "The Use of Biochemical Markers of Bone Turnover in Osteoporosis." *Osteoporosis International* 11 (0): S2–17.

Duarte, Gleison Vieira, César Faillace, and Jozélio Freire de Carvalho. 2012. "Psoriatic Arthritis." *Best Practice & Research Clinical Rheumatology* 26 (1). Elsevier Ltd: 147–56.

Duffin, Kristina Callis, Ingrid C Freeny, Steven J Schrodi, Bob Wong, Bing-Jian Feng, Razieh Soltani-Arabshahi, Tina Rakkhit, David E Goldgar, and Gerald G Krueger. 2009. "Association between IL13 Polymorphisms and Psoriatic Arthritis Is Modified by Smoking." *The Journal of Investigative Dermatology* 129 (12). Nature Publishing Group: 2777–83.

Duvallet, Emilie, Luca Semerano, Eric Assier, Géraldine Falgarone, and Marie-Christophe Boissier. 2011. "Interleukin-23: A Key Cytokine in Inflammatory Diseases." *Annals of Medicine* 43 (7): 503–11.

El Hadidi, Heba, Bahaa D.M. Grace, Tamer Gheita, and Olfat Shaker. 2008. "Involvement of IL-23 in Psoriasis and Psoriatic Arthritis Patients; Possible Role in Pathogenesis." *J Egypt Wom Dermatol Soc* 5 (2): 70–75.

Fan, J Z, X Yang, and Z G Bi. 2015. "The Effects of 6-Gingerol on Proliferation , Differentiation , and Maturation of Osteoblast-like MG-63 Cells" 48: 637–43.

Finkielstein, Vadim a., and David S. Goldfarb. 2006. "Strategies for Preventing Calcium Oxalate Stones." *Cmaj* 174 (10): 1407–9.

Finley, Don. 2012. "Cell Culture Contamination." *Biofiles*.

Florencio-silva, Rinaldo, Gisela Rodrigues, Estela Sasso-cerri, Manuel Jesus Simões, Paulo Sérgio Cerri, and Bone Cells. 2015. "Biology of Bone Tissue : Structure , Function , and Factors That Influence Bone Cells" 2015.

Garnero, P., O. Borel, and P. D. Delmas. 2001. "Evaluation of a Fully Automated Serum Assay for C-Terminal Cross-Linking Telopeptide of Type I Collagen in Osteoporosis." *Clinical Chemistry* 47 (4): 694–702.

Geboes, Lies, Laure Dumoutier, Hilde Kelchtermans, Evelien Schurgers, Tania Mitera, Jean Christophe Renauld, and Patrick Matthys. 2009. "Proinflammatory Role of the Th17 Cytokine Interleukin-22 in Collagen-Induced Arthritis in C57BL/6 Mice." *Arthritis and Rheumatism* 60 (2): 390–95.

Gheorghe, Karina Roxana, Syed Sadique, Patrick Leclerc, Helena Idborg, Ivonne Wobst, Anca Irinel Catrina, Per-Johan Jakobsson, and Marina Korotkova. 2012. "Limited Effect of Anti-Rheumatic Treatment on 15-Prostaglandin Dehydrogenase in Rheumatoid Arthritis Synovial Tissue." *Arthritis Research & Therapy* 14 (3). BioMed Central Ltd: R121.

Gladman, D D, C Antoni, P Mease, D O Clegg, and P Nash. 2005. "Psoriatic Arthritis: Epidemiology, Clinical Features, Course, and Outcome." *Annals of the Rheumatic Diseases* 64 Suppl 2: ii14–i17.

Grisar, Johannes, Peter M. Bernecker, Martin Aringer, Kurt Redlich, Markus Sedlak, Wolfgang Wolozcszuk, Susanne Spitzauer, et al. 2002. "Ankylosing Spondylitis, Psoriatic Arthritis, and Reactive Arthritis Show Increased Bone Resorption, but Differ with Regard to Bone Formation." *Journal of Rheumatology* 29 (7): 1430–36.

Guo, Yujie, Zhihong Cen, Bin Wei, Weifeng Wu, and Qiuxi Zhou. 2015. "Increased Circulating Interleukin 10-Secreting B Cells in Patients with Dilated Cardiomyopathy" 8 (December 2012): 8107–14.

Hadjidakis, Dimitrios J., and Ioannis I. Androulakis. 2006. "Bone Remodeling." *Annals of the New York Academy of Sciences* 1092: 385–96.

Helliwell, P S, and W J Taylor. 2005. "Classification and Diagnostic Criteria for Psoriatic Arthritis." *Annals of the Rheumatic Diseases* 64 Suppl 2: ii3–i8.

Holloway, Wayne R, Fiona McL Collier, Cathy J Aitken, Damian E Myers, Jason M Hodge, Mary Malakellis, Tamara J Gough, Gregory R Collier, and Geoffrey C Nicholson. 2002. "Leptin Inhibits Osteoclast Generation." *Journal of Bone and Mineral Research : The Official Journal of the American Society for Bone and Mineral Research* 17 (2): 200–209.

Igarashi, Kaoru, Je Tae Woo, and Paula H. Stern. 2002. "Effects of a Selective Cyclooxygenase-2 Inhibitor, Celecoxib, on Bone Resorption and Osteoclastogenesis in Vitro." *Biochemical Pharmacology* 63 (3): 523–32.

Ikeuchi, Hidekazu, Takashi Kuroiwa, Noriyuki Hiramatsu, Yoriaki Kaneko, Keiju Hiromura, Kazue Ueki, and Yoshihisa Nojima. 2005. "Expression of Interleukin-22 in Rheumatoid Arthritis: Potential Role as a Proinflammatory Cytokine." *Arthritis and Rheumatism* 52 (4): 1037–46.

Ji, Wei, Yajun Chen, Xia Zhao, Yunke Guo, Lingyu Zhong, Honggang Li, Dan Wang, and Yanna Song. 2015. "Beneficial Effects of Tripterygium Glycosides Tablet on Biomarkers in Patients with Ankylosing Spondylitis." *Molecular Medicine Reports* 12 (1): 684–90.

Kalinski, Pawel. 2012. "Regulation of Immune Responses by Prostaglandin E2." *Journal of Immunology (Baltimore, Md. : 1950)* 188 (1): 21–28.

Karolina, Niska, Katarzyna Pyszka, Cecylia Tukaj, Michał Woźniak, Marek Witold Radomski, and Iwona Inkielewicz-Stepniak. 2015. "Titanium Dioxide Nanoparticles Enhance Production of Superoxide Anion and Alter the Antioxidant System in Human Osteoblast Cells." *International Journal of Nanomedicine* 4 (10): 1095–1107.

Kim, Kyoung Woon, Hae Rim Kim, Jin Young Park, Jin Sil Park, Hye Jwa Oh, Yun Ju Woo, Mi Kyung Park, Mi La Cho, and Sang Heon Lee. 2012. "Interleukin-22 Promotes Osteoclastogenesis in Rheumatoid Arthritis through Induction of RANKL in Human Synovial Fibroblasts." *Arthritis and Rheumatism* 64 (4): 1015–23.

Kim, Kyoung-Woon, Hae-Rim Kim, Bo-Mi Kim, Mi-La Cho, and Sang-Heon Lee. 2015. "Th17 Cytokines Regulate Osteoclastogenesis in Rheumatoid Arthritis." *The American Journal of Pathology*, no. September. American Society for Investigative Pathology: 1–14.

Kivitz, Alan J., Luis R. Espinoza, Yvonne R. Sherrer, Maria Liu-Dumaw, and Christine R. West. 2007. "A Comparison of the Efficacy and Safety of Celecoxib 200 Mg and Celecoxib 400 Mg Once Daily in Treating the Signs and Symptoms of Psoriatic Arthritis." *Seminars in Arthritis and Rheumatism* 37 (3): 164–73.

Klein, Jonathan L., TuDung T. Nguyen, Gabriel a. Bien-Willner, Ling Chen, Kelley V. Foyil, Nancy L. Bartlett, Eric J. Duncavage, Anjum Hassan, John L. Frater, and Friederike Kreisel. 2014. "CD163 Immunohistochemistry Is Superior to CD68 in Predicting Outcome in Classical Hodgkin Lymphoma." *American Journal of Clinical Pathology* 141 (3): 381–87.

Klingberg, Eva, Merja Nurkkala, Hans Carlsten, and Helena Forsblad-D'Elia. 2014. "Biomarkers of Bone Metabolism in Ankylosing Spondylitis in Relation to Osteoproliferation and Osteoporosis." *Journal of Rheumatology* 41 (7): 1349–56.

Kontoyiannis, D, M Pasparakis, T T Pizarro, F Cominelli, and G Kollias. 1999. "Impaired On/off Regulation of TNF Biosynthesis in Mice Lacking TNF AU-Rich Elements: Implications for Joint and Gut-Associated Immunopathologies." *Immunity* 10 (3): 387–98.

Kwon, Seong Ryul, Mie Jin Lim, Chang Hee Suh, Shin Goo Park, Yeon Sik Hong, Bo Young Yoon, Hyoun Ah Kim, Hyo Jin Choi, and Park Won. 2012. "Dickkopf-1 Level Is Lower in Patients with Ankylosing Spondylitis than in Healthy People and Is Not Influenced by Anti-Tumor Necrosis Factor Therapy." *Rheumatology International* 32 (8): 2523–27.

Lafzi, Ardeshir, Surena Vahabi, Shadab Ghods, and Maryam Torshabi. 2015. "In Vitro Effect of Mineralized and Demineralized Bone Allografts on Proliferation and Differentiation of MG-63 Osteoblast-like Cells." *Cell and Tissue Banking*. Springer Netherlands.

Lau, Sean K, Peiguo G Chu, and Lawrence M Weiss. 2004. "A Specific Marker of Macrophages in Paraffin-Embedded Tissue Samples." *American Journal of Clinical Pathology*, 794–801.

Lian, J B, and G S Stein. 1995. "Development of the Osteoblast Phenotype: Molecular Mechanisms Mediating Osteoblast Growth and Differentiation." *The Iowa Orthopaedic Journal* 15: 118–40.

Lin, Linxue, Runsong Hao, Wei Xiong, and Jian Zhong. 2014. “Quantitative Analyses of the Effect of Silk Fibroin/nano-Hydroxyapatite Composites on Osteogenic Differentiation of MG-63 Human Osteosarcoma Cells.” *Journal of Bioscience and Bioengineering* 119 (5). Elsevier Ltd: 591–95.

Michalak-Stoma, Anna, Aldona Pietrzak, Jacek C. Szepietowski, Anna Zalewska-Janowska, Tomasz Paszkowski, and Grazyna Chodorowska. 2011. “Cytokine Network in Psoriasis Revisited.” *European Cytokine Network* 22 (4): 160–68.

Mitra, Anupam, Smriti K Raychaudhuri, and Siba P Raychaudhuri. 2012. “Functional Role of IL-22 in Psoriatic Arthritis.” *Arthritis Research & Therapy* 14 (2). BioMed Central Ltd: R65.

Muntean, Laura, Marena Rojas-Vargas, Pilar Font, Siao-Pin Simon, Simona Rednic, Ruxandra Schiotis, Simona Stefan, Maria M Tamas, Horatiu D Bolosiu, and Eduardo Collantes-Estévez. 2011. “Relative Value of the Lumbar Spine and Hip Bone Mineral Density and Bone Turnover Markers in Men with Ankylosing Spondylitis.” *Clinical Rheumatology* 30 (5): 691–95.

Nikoopour, Enayat, Stacey M. Bellemore, and Bhagirath Singh. 2014. “IL-22, Cell Regeneration and Autoimmunity.” *Cytokine*. Elsevier Ltd, 1–8.

Osteoblast, Fetal, and Cell Line. 2015. “Quercus Infectoria Gall Extract Enhanced the Proliferation and Activity of Human” 22 (1): 12–22.

Pinzone, Joseph J, Brett M Hall, Nanda K Thudi, Martin Vonau, Ya-wei Qiang, Thomas J Rosol, John D Shaughnessy, and John D Shaughnessy Jr. 2014. “The Role of Dickkopf-1 in Bone Development , Homeostasis , and Disease Review Article The Role of Dickkopf-1 in Bone Development , Homeostasis , and Disease” 113 (3): 517–25.

Przekora, a, and G Ginalska. 2015. “Enhanced Differentiation of Osteoblastic Cells on Novel Chitosan/ β -1,3-Glucan/bioceramic Scaffolds for Bone Tissue Regeneration.” *Biomedical Materials* 10 (1). IOP Publishing: 015009.

Przepiera-Będzak, Hanna, Katarzyna Fischer, and Marek Brzosko. 2015. “Serum IL-6 and IL-23 Levels and Their Correlation with Angiogenic Cytokines and Disease Activity in Ankylosing Spondylitis, Psoriatic Arthritis, and SAPHO Syndrome.” *Mediators of Inflammation* 2015. Hindawi Publishing Corporation: 1–7.

Raggatt, Liza J., and Nicola C. Partridge. 2010. “Cellular and Molecular Mechanisms of Bone Remodeling.” *Journal of Biological Chemistry* 285 (33): 25103–8.

Rhind, S G, G a Gannon, M Suzui, R J Shephard, and P N Shek. 1999. “Indomethacin Inhibits Circulating PGE2 and Reverses Postexercise Suppression of Natural Killer Cell Activity.” *The American Journal of Physiology* 276 (5 Pt 2): R1496–1505.

Ruiz, Danilo Garcia, Mário Newton Leitão De Azevedo, and Omar Lupi. 2012. “HLA-B27 Frequency in a Group of Patients with Psoriatic Arthritis” 1 (6): 847–50.

Rutz, Sascha, Céline Eidenschenk, and Wenjun Ouyang. 2013. “IL-22, Not Simply a Th17 Cytokine.” *Immunological Reviews* 252 (1): 116–32.

Sabat, Robert, Ellen Witte, Katrin Witte, and Kerstin Wolk. 2013. “IL-17, IL-22 and Their Producing Cells: Role in Inflammation and Autoimmunity.” *Progress in Inflammation Research*, 11–36.

Samoszuk, Michael, Michael Leuther, and Nicholas Hoyle. 2008. “Role of Serum P1NP Measurement for Monitoring Treatment Response in Osteoporosis.” *Biomarkers in Medicine* 2 (5): 495–508.

Shami, Annelie, Anki Knutsson, Pontus Dunér, Uwe Rauch, Eva Bengtsson, Christoffer Tengryd, Vignesh Murugesan, et al. 2015. “Dystrophin Deficiency Reduces Atherosclerotic Plaque Development in ApoE-Null Mice.” *Scientific Reports* 5. Nature Publishing Group: 13904.

Srirangan, S., and E. H. Choy. 2010. “The Role of Interleukin 6 in the Pathophysiology of Rheumatoid Arthritis.” *Therapeutic Advances in Musculoskeletal Disease* 2 (5): 247–56.

Stupack, Dwayne G, and David a Cheresh. 2002. “Get a Ligand, Get a Life: Integrins, Signaling and Cell Survival.” *Journal of Cell Science* 115 (Pt 19): 3729–38.

Sun, Xin-Yuan, Jian-Ming Ouyang, Ai-Jie Liu, Yi-Ming Ding, and Qiong-Zhi Gan. 2015. “Preparation, Characterization, and in Vitro Cytotoxicity of COM and COD Crystals with Various Sizes.” *Materials Science and Engineering: C* 57. Elsevier B.V.: 147–56.

Tackey, E, P E Lipsky, and G G Illei. 2004. “Rationale for Interleukin-6 Blockade in Systemic Lupus Erythematosus.” *Lupus* 13 (5): 339–43.

Taylan, Ali, Ismail Sari, Baris Akinci, Safak Bilge, Didem Kozaci, Servet Akar, Ayfer Colak, Hulya Yalcin, Necati Gunay, and Nurullah Akkoc. 2012. “Biomarkers and Cytokines of Bone Turnover: Extensive Evaluation in a Cohort of Patients with Ankylosing Spondylitis.” *BMC Musculoskeletal Disorders* 13 (1). BMC Musculoskeletal Disorders: 191.

Taylan, Ali, Ismail Sari, Didem L. Kozaci, Arif Yuksel, Safak Bilge, Yasar Yildiz, Gulten Sop, Isil Coker, Necati Gunay, and Nurullah Akkoc. 2012. “Evaluation of the T Helper 17 Axis in Ankylosing Spondylitis.” *Rheumatology International* 32 (8): 2511–15.

Teng, Michele W L, Edward P Bowman, Joshua J McElwee, Mark J Smyth, Jean-Laurent Casanova, Andrea M Cooper, and Daniel J Cua. 2015. “IL-12 and IL-23 Cytokines: From Discovery to Targeted Therapies for Immune-Mediated Inflammatory Diseases.” *Nature Medicine* 21 (7): 719–29.

Thermo Fisher Scientific. 2011. “NanoDrop: Assessment of Nucleic Acid Purity.” *Protocols and Product Manuals*, no. 042: 1–2.

Tive, L. 2000. “Celecoxib Clinical Profile.” *Rheumatology (Oxford, England)* 39 Suppl 2: 21–28; discussion 57–59.

Ustun, N, F Tok, U Kalyoncu, S Motor, R Yuksel, Yagiz Ae, H Guler, and Turhanoglu Ad. 2014. "Sclerostin and Dkk-1 in Patients with Ankylosing Spondylitis." *Acta Reumatológica Portuguesa* 39: 146–51.

Van Bezooijen, Rutger L, Bernard a J Roelen, Annemieke Visser, Lianne van der Wee-Pals, Edwin de Wilt, Marcel Karperien, Herman Hamersma, Socrates E Papapoulos, Peter ten Dijke, and Clemens W G M Löwik. 2004. "Sclerostin Is an Osteocyte-Expressed Negative Regulator of Bone Formation, but Not a Classical BMP Antagonist." *The Journal of Experimental Medicine* 199 (6): 805–14.

Van Duivenvoorde, Leonie M., van Tok, Melissa N., Baeten, Dominique L. 2013. "Membrane-Bound TNF Drives Axial and Peripheral Inflammation and Pathologic New Bone Formation." *Arthritis and Rheumatism*, no. 65.

Vasikaran, S., R. Eastell, O. Bruyère, a. J. Foldes, P. Garnero, a. Griesmacher, M. McClung, et al. 2011. "Markers of Bone Turnover for the Prediction of Fracture Risk and Monitoring of Osteoporosis Treatment: A Need for International Reference Standards." *Osteoporosis International* 22 (2): 391–420.

Wanders, Astrid, Désirée Van Der Heijde, Robert Landewé, Jéhan-Michel Béhier, Andrei Calin, Ignazio Olivieri, Henning Zeidler, and Maxime Dougados. 2005. "Nonsteroidal Antiinflammatory Drugs Reduce Radiographic Progression in Patients with Ankylosing Spondylitis: A Randomized Clinical Trial." *Arthritis and Rheumatism* 52 (6): 1756–65.

Wilson, Floranne C, Murat Icen, Cynthia S Crowson, Marian T McEvoy, Sherine E Gabriel, and Hilal Maradit Kremers. 2009. "Incidence and Clinical Predictors of Psoriatic Arthritis in Patients with Psoriasis: A Population-Based Study." *Arthritis and Rheumatism* 61 (2): 233–39.

Wolk, Kerstin, Ellen Witte, Elizabeth Wallace, Wolf Dietrich Döcke, Stefanie Kunz, Khusru Asadullah, Hans Dieter Volk, Wolfman Sterry, and Robert Sabat. 2006. "IL-22 Regulates the Expression of Genes Responsible for Antimicrobial Defense,

Cellular Differentiation, and Mobility in Keratinocytes: A Potential Role in Psoriasis." *European Journal of Immunology* 36 (5): 1309–23.

Wong, Marisa L, and Juan F Medrano. 2005. "One-Step Versus Two-Step Real- Time PCR" 39 (1): 75–85.

Yang, Xuyan, and Song Guo Zheng. 2014. "Interleukin-22: A Likely Target for Treatment of Autoimmune Diseases." *Autoimmunity Reviews* 13 (6). Elsevier B.V.: 615–20.

Ye, Jian, George Coulouris, Irena Zaretskaya, Ioana Cutcutache, Steve Rozen, and Thomas L Madden. 2012. "Primer-BLAST: A Tool to Design Target-Specific Primers for Polymerase Chain Reaction." *BMC Bioinformatics* 13 (1): 134.

Zhang, Lei, Yong-gang Li, Yu-hua Li, Lei Qi, Xin-guang Liu, Cun-zhong Yuan, Nai-wen Hu, et al. 2012. "Increased Frequencies of Th22 Cells as Well as Th17 Cells in the Peripheral Blood of Patients with Ankylosing Spondylitis and Rheumatoid Arthritis." *PLoS ONE* 7 (4): e31000.

Zheng, Yan, Dimitry M Danilenko, Patricia Valdez, Ian Kasman, Jeffrey Eastham-Anderson, Jianfeng Wu, and Wenjun Ouyang. 2007. "Interleukin-22, a T(H)17 Cytokine, Mediates IL-23-Induced Dermal Inflammation and Acanthosis." *Nature* 445 (7128): 648–51.

ANNEX I

Table I – CASPAR criteria (Adapted from Amherd-Hoekstra et al 2010).

Criterion	Points
1. Evidence for psoriasis	
Current psoriasis present	2 points
Positive personal history	1 point
Positive family history	1 point
2. Nail psoriasis	1 point
3. Rheumatoid factor not detectable	1 point
4. Dactylitis	
Current dactylitis	1 point
5. Radiologic detection of ossification in proximity to joints	1 point

Table II – Primers used for RT-PCR.

Gene	Gene name	Sequence	AT	Transcript
RANK	Receptor activator of NF-KB	Fw: GAACATCATGGGACAGAGAAATC	60°C	89 bp
		Rv: GGCAAGTAAACATGGGGTTC		
CTSK	Cathepsin K	Fw: GCCAGACAACAGATTTCCATC	60°C	75 bp
		Rv: CAGAGCAAAGCTCACCACAG		
CSF1R	Colony stimulating factor 1 receptor	Fw: GAACATCCACCTCGAGAAGAAA	60°C	88 bp
		Rv: GACAGGCCTCATCTCCACAT		
NFATc1	Nuclear factor of activated T cells cytoplasmic 1	Fw: GCAAGCCGAATTCTCTGGTG	60°C	144 bp
		Rv: TACCGTTGGCGGGAAGGTAG		
18S rRNA	Ribossomal ribonucleic acid	Fw: GGAGTATGGTTGCAAAGCTGA	60°C	129 bp
		Rv: ATCTGTCAATCCTGTCCGTGT		

AT – Annealing temperature

ANNEX II

Genotyping protocol for membrane bound TNF mice

PCR

Take along a H_2O control and a positive and negative control (from a previous screen)

Needed for 1 sample:

Buffer 5x	4 µL	
H_2O	13.2 µL	
10 mM dNTP	0.4 µL	
5 µM forward TNF primer	0.6 µL	
5 µM reverse TNF primer	0.6 µL	
Phusion DNA polymerase	0.2 µL	
Total:	19 µL	+ 1 µL DNA sample + 3µL loading buffer

PCR programme:

30 sec	98 °C	
10 sec	98 °C	
10 sec	60 °C	
12 sec	72 °C	go back to step 2 for 35 times
5 min	72 °C	
∞	4 °C	

Expected bands: ~ 600-700 bp Het

~ 1000 bp WT

Diluted ladder: 1:4 (1 µL stock + 3 µL H_2O)

Apply 10 µL per well in agarose gel

1% agarose gel (80 mL TBE 0.5X + 0.8 g agarose + 1.5 µL Red Safe)

Parameters: 80V during 1h10min

ANNEX III

Immunohistochemistry CD3 for paraffin blocks

1. Desparaffinization and hydration
   a. 15 min in xylene
   b. 10 min in ethanol 100%
   c. 10 min in ethanol 96%
   d. 10 min in ethanol 70%
   e. 5 min in distilled water
   f. Delimit the perimeter with hydrophobic pen

2. Antigenic retrieval
   a. 20 min at 37°C with proteinase K (1 mL/ slide) – working solution
   b. 10 min at RT
   c. Washings 2x 5 min with PBS/Triton 0.005%

3. Endogenous peroxidase blocking
   a. 30 min with 0.3% endogenous peroxidase in methanol
   b. 5 min in running water

4. Total protein block
   a. 20 min at RT PBS/BSA 1%

5. Primary antibody
   a. 150 µL/slide
   d. 1:300 in antibody diluent (negative control slide stays in PBS/Triton 0.005%)
   b. 1h at RT
   c. Washings 2x 3 min PBS/Triton 0.005%

6. Secondary antibody (HRP)
   a. 150 µL/slide Envision Rabbit
   b. 20 min at RT

c. Washings 2x 3min PBS/Triton 0.005%

7. Developing solution

a. 5 min DAB – 20 µL chromogen + 1 mL substrate

b. Washings 2-3 min in distilled water

8. Hematoxylin contrast

a. Hematoxylin 10 sec

b. Washings in hot running water 3-5 min

c. Ethanol 70% 30 sec

d. Ethanol 96% 30 sec

e. Ethanol 100% 30 sec

f. Xilene 15 min

g. Slide mounting with proper mounting medium

Proteinase K Solution (20 µg/mL in TE Buffer, pH 8.0):

TE Buffer (50 mM Tris Base, 1 mM EDTA, 0.5% Triton X-100, pH 8.0):

Tris Base ---------- 6.10 g
EDTA ---------- 0.37 g
Triton X-100 ---------- 5 mL
Distilled water ---------- 1000 mL

Mix to dissolve. Adjust pH 8.0 using concentrated HCl (10N HCl). Store at room temperature.

Proteinase K **Stock Solution** (40x, 400 µg/mL or 12 units/mL):

Proteinase K (30 units/mg)---------- 0.0043 g (4.3 mg)

TE Buffer, pH 8.0 ---------- 5 mL

Glycerol ---------- 5 mL

Add proteinase K to TE buffer until dissolved. Then add glycerol and mix well. Aliquot and store at –20ºC for 2-3 years.

Working Solution (1x, 20 µg/mL or 0.6 units/mL):

Proteinase K Stock Solution (40x) ------ 0.6 mL
TE Buffer, pH 8.0 ---------- 19.4 mL

ANNEX IV

Table I – Demographic and clinical table of PsA and AS patients for IL-22, IL-23 and PGE_2 assays.

	Healthy	PsA patients	AS patients	*p* value
N	12	26	6	
Age (years)	35.5 [33.25-43.75]	48.5 [34-60]	42 [31.75-49]	0.0681
Male (%)	58.3%	62%	50%	0.5772
Symptoms duration (years)	NA	2.5 [0.81-5]	13.50 [5-26.5]	0.0323
Axial involvement (% yes)	NA	57%	75%	0.3878
Peripheral involvement (% yes)	NA	79%	25%	0.042
Entheseal involvement (% yes)	NA	64%	0%	
HLA-B27 (% positive)	NA	16%	50%	0.0845
NSAIDs (% yes)	NA	0%	50%	
NSAIDs duration (months)	NA	0	3 [3-58]	
DMARDs (% yes)	NA	11.1%	0%	
Bisphosphonates (% yes)	NA	0%	0%	
Anti-TNF (% yes)	NA	0%	33%	
ESR (mm/h)	NA	16 [8-37]	20.5 [13.5-36.5]	0.2722
CRP (mg/L)	NA	5 [1.08-11.75]	4.15 [2.15-7.6]	0.8275

Results are expressed in median [interquartile range 25-75]. *p* values lower than 0.05 are considered statistically significant. PsA – psoriatic arthritis; AS – ankylosing spondylitis; NA – not applicable; NSAIDs – non-steroidal anti-inflammatory drugs; DMARDs – disease-modifying anti-rheumatic drugs; ESR – erythrocyte sedimentation rate; CRP – C-reactive protein.

ANNEX V

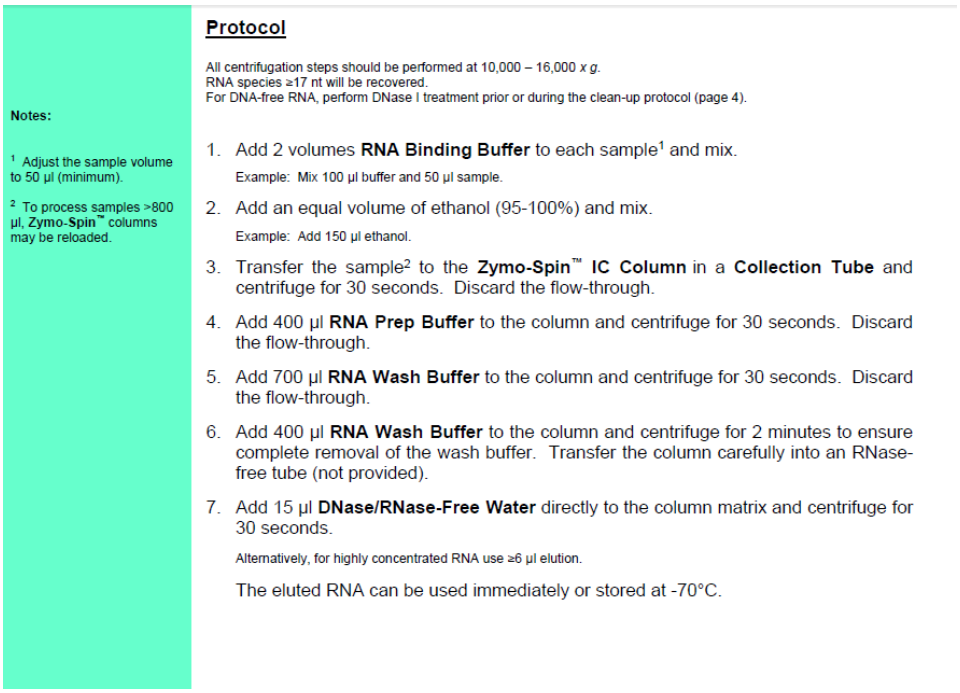

Protocol

All centrifugation steps should be performed at 10,000 – 16,000 *x g*.
RNA species ≥17 nt will be recovered.
For DNA-free RNA, perform DNase I treatment prior or during the clean-up protocol (page 4).

Notes:

[1] Adjust the sample volume to 50 µl (minimum).

[2] To process samples >800 µl, Zymo-Spin™ columns may be reloaded.

1. Add 2 volumes **RNA Binding Buffer** to each sample[1] and mix.
   Example: Mix 100 µl buffer and 50 µl sample.
2. Add an equal volume of ethanol (95-100%) and mix.
   Example: Add 150 µl ethanol.
3. Transfer the sample[2] to the **Zymo-Spin™ IC Column** in a **Collection Tube** and centrifuge for 30 seconds. Discard the flow-through.
4. Add 400 µl **RNA Prep Buffer** to the column and centrifuge for 30 seconds. Discard the flow-through.
5. Add 700 µl **RNA Wash Buffer** to the column and centrifuge for 30 seconds. Discard the flow-through.
6. Add 400 µl **RNA Wash Buffer** to the column and centrifuge for 2 minutes to ensure complete removal of the wash buffer. Transfer the column carefully into an RNase-free tube (not provided).
7. Add 15 µl **DNase/RNase-Free Water** directly to the column matrix and centrifuge for 30 seconds.
   Alternatively, for highly concentrated RNA use ≥6 µl elution.

The eluted RNA can be used immediately or stored at -70°C.

Protocol excerpt from Zymo Research, RNA Clean-up & Concentration Protocol